A Surface-Wind Speed Conversion Technique Using WSR-88D Doppler Weather Radar Velocity Data During Tropical Cyclone Landfall Events

Stacy R. Stewart
Adjunct Professor
Embry-Riddle Aeronautical University, Daytona Beach, Florida
(Retired Senior Hurricane Specialist
NOAA-National Hurricane Center, Miami, Florida)

1. INTRODUCTION

Estimating the intensity of tropical cyclones (TC) is difficult for forecasters given the amount of limited in situ wind speed data from sources such as reconnaissance aircraft flight-level winds and stepped-frequency microwave radiometer (SFMR) near-surface winds, drone aircraft flight-level wind data, surface wind observations, space-borne scatterometers and synthetic aperture radars, and reconnaissance aircraft- and ground-based Doppler weather radar velocity data. Of the aforementioned wind data sampling platforms, only ground-based Doppler radars can sample a TC's wind field on time scales that can produce a 2-dimensional tangential wind field almost continuously owing to its much finer time sampling periods (e.g., <5 min NOAA WSR-88D Doppler radar), while also detecting transient mesoscale and even tornadic-scale wind features that must be filtered out of the background wind flow. One drawback with land-based Doppler radars, however, is that by the time a TC comes within range, the system is typically within 24 h of making landfall, limiting the radar's usefulness in the operational TC forecast and watch-warning processes. However, land-based Doppler weather surveillance radars still have significant utility in the TC operational- and post-analysis processes.

For the past seven decades, reconnaissance aircraft have provided the bulk of wind data that have been used to estimate the intensity of tropical cyclones (TC). However, this indispensable *in situ* information has provided little more than snapshots in time and space of tropical cyclones' intensity and wind field structure, and generally at altitudes of approximately 300, 800, 1500, and 3,000 meters above sea level (ASL) or 975-, 925-, 850-, and 700-hPa pressure levels, respectively. Various remote sensing platforms such as space-borne scatterometers (e.g., ASCAT) and microwave radiometers (e.g., SSMI/S) can provide much more detailed wind data about a TC's entire near-surface (i.e., 10-meters altitude above sea level) wind field, but these data are gathered infrequently and cannot resolve peak intensities above approximately 80 kt (41 ms^{-1}) due the relatively coarse field-of-view resolution (12.5 – 50 km) of the various instruments.

By contrast, land-based WSR-88D Doppler weather surveillance radars operated by the U.S. National Weather Service can provide a complete depiction of a TC's wind field at multiple altitudes, albeit at relatively short distances from populated coastlines, by utilizing the Doppler velocity data. Stewart and Lyons (1995) were the first to document the use of WSR-88D Doppler velocity data to estimate the intensity of a tropical cyclone when they analyzed western North Pacific Tropical Cyclone Ed as the eventual Super Typhoon approached and moved across the island of Guam on 30 September 1993; these data were also implemented operationally by Joint Typhoon Warning Center (JTWC) — Guam forecasters (JTWC ATCR 1993). Land-based Doppler radars can aid forecasters by filling in the gaps between the narrow aircraft flight legs, along with temporal changes in the structure of a TC's horizontal and vertical wind fields, especially the radius of maximum winds (RMW).

2. METHODOLOGY OF THE 4-BIN AVERAGE (4BAV) DOPPLER VELOCITY VALUE TECHNIQUE

Although Doppler weather radars can only measure winds that contain a component of motion toward or away from the radar site (i.e., radial velocities), those velocity values indicate at least the minimum wind speed present at any location within the cyclone. However, when the wind direction is aligned parallel to the radar beam, then the Doppler velocity measured is also the actual wind speed (V_{ACTUAL}) at that altitude.

Reconnaissance aircraft sample winds along a very narrow flight path, whereas Doppler weather radar data are collected within a relatively large and contiguous volume sample that increases in size with increasing range. The surveillance aircraft typically collect peak 10-second wind data along approximately 1-km-long flight track segments; WSR-88D Doppler data are collected in 250-m long radial bins along 360 azimuthal directions (Fig. 1).

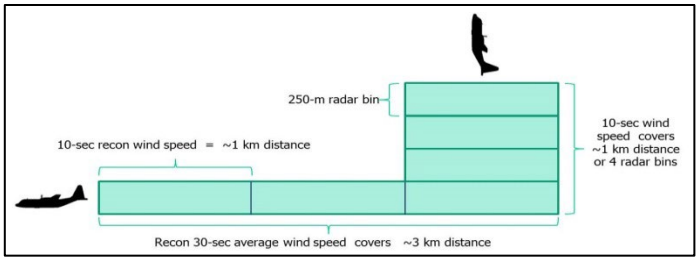

Figure 1. Schematic of the 4-bin average (4BAV) Doppler velocity value concept.

To approximate the 1-km-long flight leg segments, WSR-88D Doppler radar velocity data were averaged along four (4) contiguous 250-m radial bins yielding a 4-bin average Doppler velocity value. The peak Doppler velocity value is first located, followed by three contiguous velocity values that will yield the highest $4BAV_{DOPPLER}$ value (Fig 2).

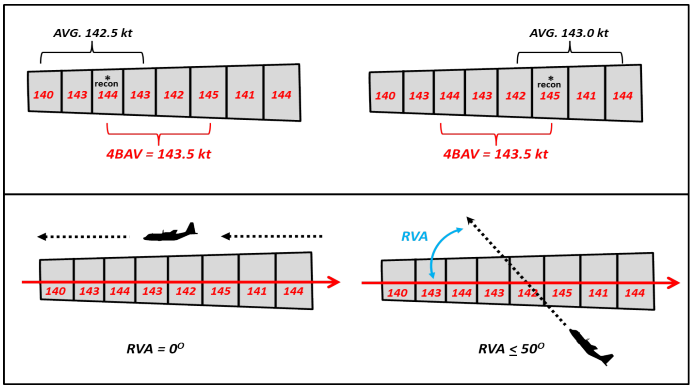

Figure 2. Schematic of a 4-bin average Doppler velocity (4BAV) used to convert to a V_{ACTUAL} wind speed value (top panel). Notice that when RVAs exceed 50°, the aircraft might only sample one or two radar bins of velocity data instead of four bins (bottom panel).

The 4BAV value was then divided by the cosine of the angular difference between the aircraft-derived 30-s wind direction and the radar radial azimuth, referred to as the Radar Viewing Angle (RVA), yielding an environmental wind speed (V_{ACTUAL}) or the tangential velocity ($V_{TANGENTIAL}$) of a tropical cyclone (Fig. 3).

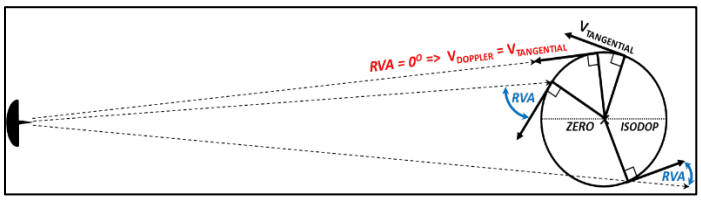

Figure 3. Schematic of various Doppler radar (velocity) viewing angles (RVA). When the RVA is 0° (i.e., radar radial directly along the actual wind direction), $V_{DOPPLER}$ equals V_{ACTUAL} (or $V_{TANGENTIAL}$).

The V_{ACTUAL} values were then compared to and linearly correlated with the corresponding aircraft-derived 10-second average wind speeds. In an attempt to replicate an aircraft's flight path along four contiguous radar bins, RVAs were limited to angles ≤50°. While this value may appear to be large, the data set would have contained less than 10 samples if RVAs had been limited to near zero-degree angle, resulting in an almost meaningless data comparison. By contrast, extending the RVAs to at least 50° resulted in 135 data samples from the seven hurricanes of various intensities that were examined.

3. DATA SET AND STATISTICAL ANALYSIS OF 4BAV-DERIVED WIND SPEEDS

WSR-88D radar collection times for seven U.S. landfalling hurricanes during the period 2004-2022 – Charley (2004), Ivan (2004), Katrina (2005), Wilma (2005), Harvey (2017), Dorian (2019), and Ian (2022) -- were limited to within ±1.5 minutes of the reconnaissance aircraft wind observation time and within ±250 m (820 ft) of the aircraft flight-level altitude. Despite the non-concurrent aircraft and radar data sampling times and altitudes resulting in a non-homogeneous data set, an impressive correlation coefficient of 0.99 of the 135 samples was still obtained, along with a relatively small root-mean square error (RMSE) of 3.69 kt (Fig. 4). This indicates excellent fidelity between the aircraft-derived flight-level wind speeds and the radar-derived 4BAV-derived V_{ACTUAL} wind speeds.

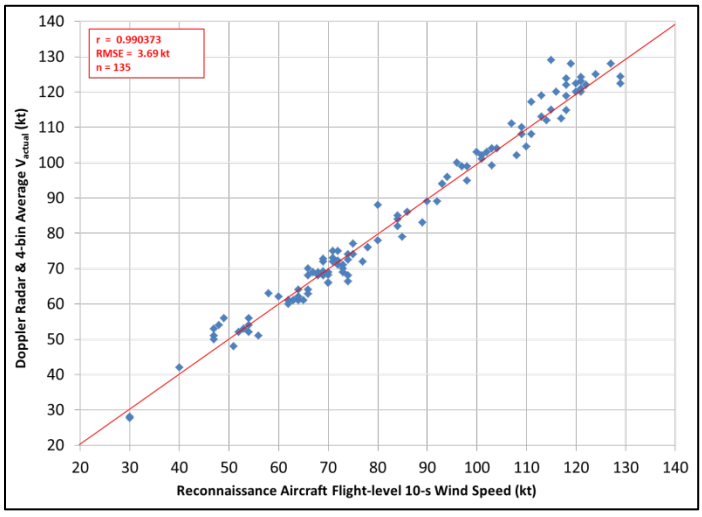

Figure 4. Plot of aircraft 10-second-average flight-level wind speeds (kt) versus V_{ACTUAL} wind speeds (kt) derived from the 4BAV technique. Red line represents a perfect data fit.

Users of the $4BAV_{DOPPLER}$ technique may be concerned about the sensitivity of computing RVAs and resultant cosines of those angular values. Table 1 indicates that even for RVAs ≤15°, $V_{TANGENTIAL}$ errors would only be ±3 kt for $V_{DOPPLER}$ values ≤90 kt and only ±5 kt for $V_{DOPPLER}$ values (hereafter $4BAV_{ACTUAL}$) of 100-150 kt.

$4BAV_{DOPPLER}$ (kt) Conversion to $V_{TANGENTIAL}$ (kt) for Various Radar Viewing Angles (RVA)												
$4BAV_{DOPPLER}$ (kt) / RVA	5°	10°	15°	20°	25°	30°	35°	40°	45°	50°	55°	60°
20									28	31	35	40
30			31	32	33	35	37	39	42	47	52	60
40		41	41	43	44	46	49	52	57	62	70	80
50		51	52	53	55	58	61	78	71	78	87	100
60		61	62	64	66	69	73	78	85	93	105	120
70		71	72	74	77	81	85	91	99	109	122	140
80		81	83	85	88	92	98	104	113	124	139	160
90		91	93	96	99	104	110	117	127	140	157	180
100		102	104	106	110	115	122	131	141	156	174	200
110		112	114	117	121	127	134	144	156	171	192	220
120		122	124	128	132	139	146	157	170	187	209	240
130		132	135	138	143	150	159	170	184	202	227	260
140	141	142	145	149	154	162	171	183	198	218	244	
150	151	152	155	160	177	173	183	196	212	233	262	

Table 1. Nomogram of $V_{TANGENTIAL}$ (V_{ACTUAL}) wind speeds (kt) as a function of $4BAV_{DOPPLER}$ velocity values (kt) and Radar Viewing Angles (RVA).

Once the $4BAV_{ACTUAL}$ wind speeds have been converted to $V_{TANGENTIAL}$ wind speeds, the next concern is how to convert those latter values to equivalent surface wind (ESW) speeds. For more than two decades, the National Hurricane Center (NHC) has been using eyewall reduction factors of 0.90, 0.80, and 0.75 at flight-level pressure values of 700 hPa, 850 hPa, and 925 hPa, respectively (Table 2). These reduction or adjustment factors were based on a dropwindsonde data analysis performed by Franklin et al (2003) on 630 total profiles, of which 429 were eyewall profiles, from 1997-99 and which covered an intensity range of 65 to 155 kt (33–80 ms^{-1}). Despite the relatively large number of sondes released in the eyewalls, there was no mention of the eyewall structure (e.g., rainfall rates or radar reflectivity) in their report. In regions of weak radar equivalent reflectivity values (e.g., ≤25 dBZ_e), one would expect weak downdrafts to be collocated that could result in reduction values less than those shown in Table 2.

Flight level	Eyewall	Outer Vortex (convection)	Outer Vortex (not in convection)
700 hPa	0.90	0.85	0.80
850 hPa	0.80	0.80	0.75
925 hPa	0.75	0.75	0.75
1000 ft (305 m)	0.80	0.80	0.80

Table 2. Reconnaissance aircraft flight-level-to-surface (10 m ASL) wind speed adjustment factors (From Franklin et al 2003, their Table 2).

In order to determine if the aforementioned adjustment factors were applicable in the storm cases presented in section 4 of this paper, a comparison of coincident WSR-88D radar equivalent reflectivity values (dBZ) with the associated dropwindsonde adjustment factor was made. The locations of the 630 sondes used to derive the Franklin et al (2003) flight-level-to-surface wind adjustment factors shown in Table 2 are displayed in Figure 5, (Franklin et al 2003 their Figure 1). However, of the 429 eyewall dropwindsonde profiles used in their

study, only 13 profiles from hurricanes Georges (1998), Bonnie (1998), Dennis (1999), and Lenny (1999) were within range of WSR-88D Doppler weather radars.

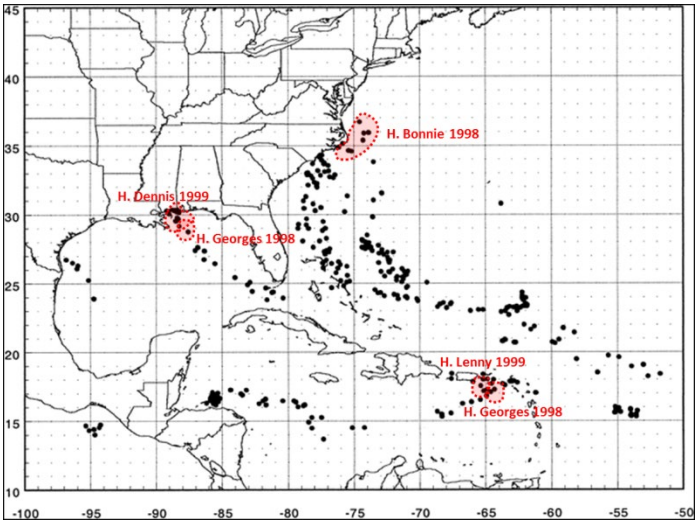

Figure 5. Locations of the 630 dropsondes used to derive the adjustment factors shown in Table 2 (from Franklin et al 2003). Red-shaded areas show locations of eyewall dropsondes collocated with WSR-88D Doppler weather radar reflectivity data.

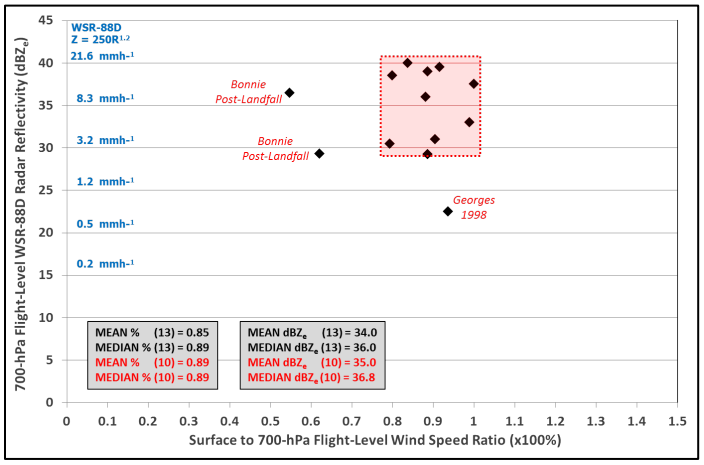

Figure 6. Plot of eyewall surface- to 700-hPa flight-level wind-speed ratios versus 4-bin-average radar reflectivity (dBZ_e) values. Reflectivity datum was collected within ±985 ft (±300 m) of the flight-level RMW altitude (ft).

Similar to the 4BAV technique, a 4-bin average of radar equivalent reflectivity values (dBZ_e) at the flight-level (~700 hPa) dropsonde release point was computed, and which was then converted to an equivalent rainfall rate utilizing the WSR-88D Doppler radar tropical rainfall rate algorithm, $Z_e = 250R^{1.4}$, where, Z_e is radar equivalent reflectivity (mm^6m^{-1}) and R is rainfall rate (mmh^{-1}). Those dBZ_e values were then compared to the ratio of the 700-hPa flight-level wind speed and surface wind speed (kt) as per Franklin et al (2003). However, due to a few dropsondes not reporting a surface wind, in those cases, the wind-speed that was reported within 2 hPa of the surface pressure was used to compute the wind-speed ratio in order to keep the small data sample from being reduced further. The wind-speed ratio was calculated by dividing by the surface wind speed (kt) by flight-level RMW wind speed (kt).

An analysis of the 13 dropsonde profiles indicates that there is a clustering of values around the 700-hPa flight-level reduction factor of 0.90. There were three outlier profiles associated with hurricanes Bonnie and Georges. In the two Bonnie cases, the dropsonde sampling occurred a few hours after the hurricanes had passed over eastern North Carolina with the low-level circulation having been disrupted due to land interaction, resulting in a weaker near-surface wind field than if the storm had remained over open-ocean. In the Georges' case, the sonde release point was about 200 m from an adjacent band of higher reflectivity values of 40-45 dBZ_e that the hurricane rainband was moving towards. Given that the radar data were collected about 1.5 min before the time of the sonde release time, it is probable that the dropwindsonde fell through that band of higher reflectivity values.

For all cases, the median surface to 700-hPa flight-level wind speed ratio was 0.89 and the median radar reflectivity value was 36.0 dBZ_e, whereas, the 10 case-sample (after eliminating the three outlier dropsonde soundings) yielded a median surface to 700-hPa flight-level wind speed ratio of 0.89 and the median radar reflectivity value was 36.8 dBZ_e. Those wind speed adjustment factors are very close to the 0.90 adjustment factor found by Franklin et al (2003) and suggests that a minimum radar reflectivity value of ~36 dBZ_e or a rainfall rate of ~10 mmh^{-1} is required to produce enough downdraft strength to bring down higher winds aloft that will allow the utilization of the 0.90 adjustment factor.

The requirement of having significant convection in the inner core region or eyewall of a tropical cyclone in order to produce the adjustment factors shown in Table 2 was first noted in NHC's 2100 UTC 18 SEP 2003 Tropical Cyclone Discussion (TCD) for Hurricane Isabel — *"If flight-level observations were all we had, Isabel would be a category three hurricane. The hurricane hunter aircraft this afternoon found a number of spots of winds of 110-120 kt. This would normally correspond to surface winds of 100-105 kt. However, numerous dropsonde profiles in the high wind regions of the circulation show a consistent and unusually steep fall-off of wind in the boundary layer. This is consistent with the meager convection in the hurricane core. Based on these profiles...the initial intensity is set at 90 kt."* This *in situ* reconnaissance wind analysis was also described in the NHC's Hurricane Irene (2003) Tropical Cyclone Report (Beven and Cobb 2014). Collocated radar reflectivity data from the Morehead City, North Carolina, WSR-88D Doppler radar (KMHX; data not shown) indicate that an equivalent reflectivity value at the aircraft flight-level release point of the dropsonde was ~32 dBZ_e with ~29 dBZ_e echoes immediately adjacent to and upsweep from both the release and splash locations. These radar reflectivity values would tend to corroborate the findings in Figure 6 that a minimum equivalent reflectivity value of ~36 dBZ_e is needed in order to apply the 700-hPA flight-level adjustment factor of 0.90 contained in Table2.

4. APPLICATION OF THE 4BAV TECHNIQUE ON HISTORICAL ATLANTIC HURRICANES

In this study, the $4BAV_{ACTUAL}$ wind speeds were reduced to equivalent 10-meter wind speeds (kt) using the National Hurricane Center's standard reduction values of 0.80, 0.75, 0.80, and 0.90 corresponding to flight-level pressures of 975, 925, 850, and 700 hPa, respectively (Table 2), for some historical hurricanes.

a. Hurricane Katrina (2005) -- When the major hurricane was nearing landfall along the southeastern coast of Louisiana early on 29 August 2005 (Knabb et al 2023), $4BAV_{ACTUAL}$ wind data indicate that Katrina possessed 140-144 kt (72-74 ms^{-1}) at ~700-hPa near the Mouth of the Mississippi River (Fig. 7). Those $4BAV_{ACTUAL}$ values gradually spread 'onshore' and equated to equivalent 10-m wind speeds of 126-130 kt (65-67 ms^{-1}), or Category 4 strength, vice the post-analysis assessed category-3 intensity of 110 kt (56.5ms^{-1}). Associated radar equivalent reflectivity values were 45-48 dBZ_e (data not shown), an indication that strong downdrafts were likely bringing those winds

down to the surface. Katrina's central pressure at that time was ~917 hPa, which equates to an intensity of ~145 kt based on the Dvorak satellite technique pressure-wind (P-W) relationship (Velden et al 2006). That P-W relationship supports the higher estimated intensity of 126-130 kt (65-67 ms^{-1}) that are based on the $4BAV_{ACTUAL}$ wind speed values, which were also less than 1 kt (0.5 ms^{-1}) higher than the raw Doppler velocity values.

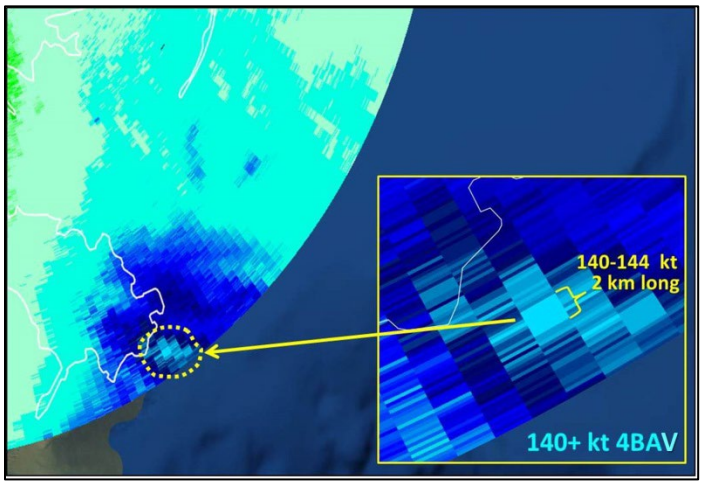

Figure 7. Katrina with a 2-km contiguous run of 140-144 kt $4BAV_{ACTUAL}$ values at ~9,350 ft (2850 m) ASL near landfall over southeastern Louisiana at 0826:48 UTC 29 AUG 2005 from KLIX-Slidell, LA WSR-88D Doppler radar. (Radar data display courtesy *grlevelx.com*)

Owing to Katrina's relatively large RMW of 33-37 km (18-20 n mi), U.S. Air Force Reserve (USAFR) and National Oceanic and Atmospheric Administration (NOAA) reconnaissance aircraft circumnavigated around and missed the stronger wind speeds as indicated by the KLIX WSR-88D Doppler radar data (Fig. 8). This type of undersampling of peak wind speeds in tropical cyclones possessing large RMWs is common (Uhlhorn and Nolan 2012).

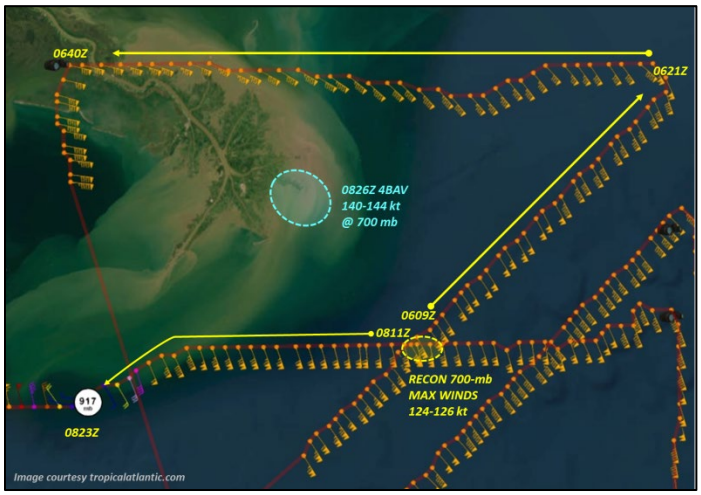

Figure 8. Depiction of the area of 140-144 kt $4BAV_{ACTUAL}$ wind speed values at 0826:48 UTC 29 AUG 2005 and the various flight tracks of an Air Force Reserve reconnaissance aircraft that circumnavigated and missed Katrina's stronger winds at the Mouth of the Mississippi River. (Reconnaissance data plot courtesy of *tropicalatlantic.com*)

That band of stronger winds maintained continuity during and after Katrina made landfall near Buras, Louisiana, but it did weaken some as Katrina turned northward and passed over Louisiana's Chandeleur Islands between 1000-1200 UTC 29 August 2005 (Fig. 9). That large area of 126-kt (65 ms_{-1}) also possessed a few embedded $4BAV_{ACTUAL}$ velocity values of 140 kt (69 ms^{-1}) that were collocated with radar equivalent reflectivity values of 40-46 dBZ_e (data not shown).

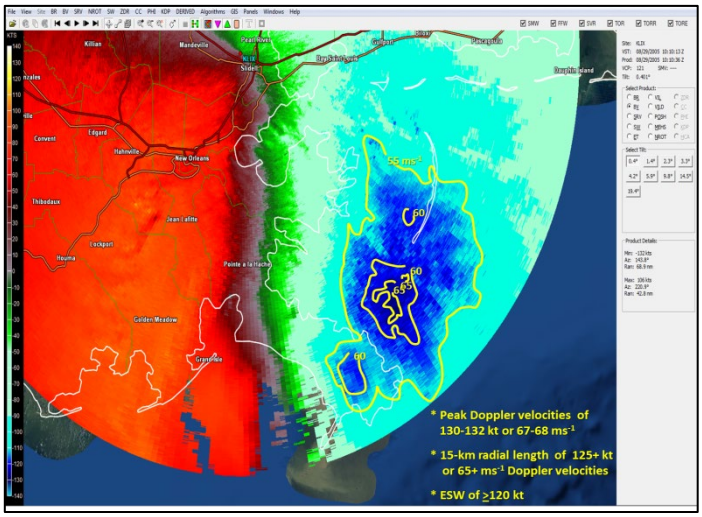

Figure 9. Radar depiction of an area of 116-126 kt $4BAV_{ACTUAL}$ wind speed values at ~8,500 ft (2600 m) ASL near Louisiana's Chandeleur Islands at 1010:36 UTC 29 AUG 2005 from KLIX-Slidell, LA WSR-88D Doppler radar. (Radar data display courtesy *grlevelx.com*)

Similar to when Katrina was approaching the southeastern coast of Louisiana ~2 h earlier, Doppler radar data from Slidell, Louisiana (KLIX) indicated that reconnaissance aircraft again circumnavigated around and missed the hurricane's stronger wind speeds aloft (Fig. 10) that are estimated to have yielded peak equivalent surface wind speeds (ESW) of ~120 kt (62 ms^{-1}).

Figure 10. Depiction of an area of 116-126 kt $4BAV_{ACTUAL}$ wind speed values at 1010:36 UTC 29 AUG 2005 and the various flight tracks of an Air Force Reserve reconnaissance aircraft that circumnavigated and Katrina's stronger winds near Louisiana's Chandeleur Islands. (Reconnaissance data plot courtesy of *tropicalatlantic.com*)

Less than 4 h after the Louisiana landfall, Katrina's eye made a third U.S. landfall near the Louisiana-Mississippi Gulf coast at 1445 UTC 29 August 2005 with a band of strong eyewall convection extending eastward about 3.4 n mi (6.2 km) offshore the Mississippi coast. This convective feature was reconnoitered by a USAFR reconnaissance aircraft from 1506:30–1509:00 UTC (Fig. 11) and revealed a streak of 700-hPa winds of 124–127 kt (64.9–65.5 ms^{-1}) that yielded ESW values of 112–114 kt (58.7–58.9 ms^{-1}) that moved onshore approximately 5 min later at 1510 UTC. The convection contained radar equivalent reflectivity values of 40-46 dBZ_e, suggestive that those stronger winds

aloft likely mixed downward to the surface within strong downdrafts using the NHC's standard 0.90 adjustment factor.

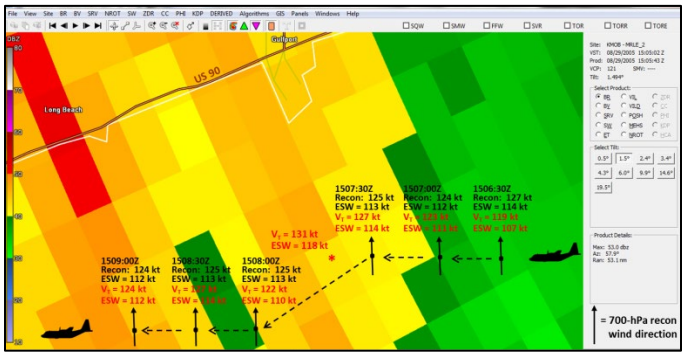

Figure 11. Mobile, AL (KMOB) WSR-88D Doppler radar reflectivity data (dBZ$_e$) at 1505:43 UTC 29 August 2005 with 1506:30-1509:00 UTC U.S. Air Force Reserve reconnaissance aircraft 700-hPa flight track (dashed black line), flight-level wind speed (kt; black text), flight-level-to-surface equivalent surface wind (ESW) speed (kt; black text), and flight-level wind direction (black arrows; true north at top of image) overlaid. The 4BAV$_{TANGENTIAL}$ winds (kt; red text) are within ±1.0 Kft (305 m) of the aircraft flight-level altitude. (Radar data display courtesy *grlevelx.com*)

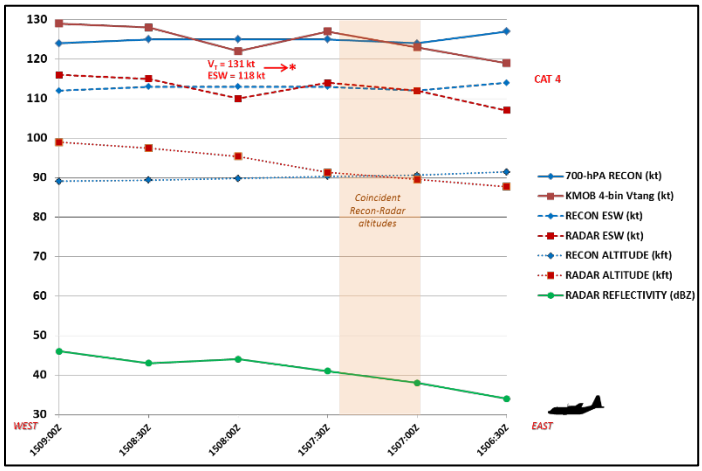

Figure 12. Time series plot of reconnaissance aircraft 700-hPa flight-level data and KMOB WSR-88D Doppler radar reflectivity (dBZ$_e$), 4BAV$_{TANGENTIAL}$ (4-bin V$_{tang}$) wind data, and radar beam centerline altitude (kft) displayed in Fig. 11 on 29 August 2005.

Coincident with the aforementioned USAFR reconnaissance flight were 4BAV$_{TANGENTIAL}$ winds speeds of 119-131 kt (61.3–65.5 ms^{-1}) that yielded ESW values of 107–118 kt (55.2–60.8 ms^{-1}) obtained from the Mobile, AL (KMOB) WSR-88D Doppler (NOTE: the KLIX WSR-88D Doppler radar was inoperable during this time) using a 0.90 adjustment factor. Although some of the Doppler radar velocity data were coincident with the aircraft flight track, most of the radar were sampled 100-900 ft (30–281 m) higher than the aircraft altitude (Fig. 12), suggesting that a slightly larger adjustment factor than 0.90 would be more appropriate. Given the proximity of that band of vigorous deep convection, it is highly probable that peak ESW values of 114–118 kt, or Category-4 winds, affected the Mississippi coast in the vicinity of Gulfport at approximately 1510–1515 UTC 29 August 2005. Unfortunately, the Gulfport-Biloxi International Airport (KGPT) and the Keesler AFB, MS (KBIX) surface observing equipment ceased functioning at 1030 UTC and 1400 UTC, respectively, and therefore could not verify those radar- and aircraft-estimated ESW speeds.

b. Hurricane Harvey (2017) – Hurricane Harvey made landfall along the Central Texas coast on San Jose Island, TX, at 0300 UTC 26 August 2017 with an estimated central pressure of 937 hPa and an intensity of 115 kt (59.3 ms^{-1}) or category-4 status according to the NOAA-NHC (Blake and Zelinsky 2018). However, the USAFR reconnaissance aircraft flight-level (Fig. 13) wind speed and stepped-frequency microwave radiometer (SFMR) near-surface (10 m) wind speed (Fig. 14) data indicated that the maximum winds at landfall were more likely ≤110 kt (56.5 ms^{-1}) or Category-3 strength.

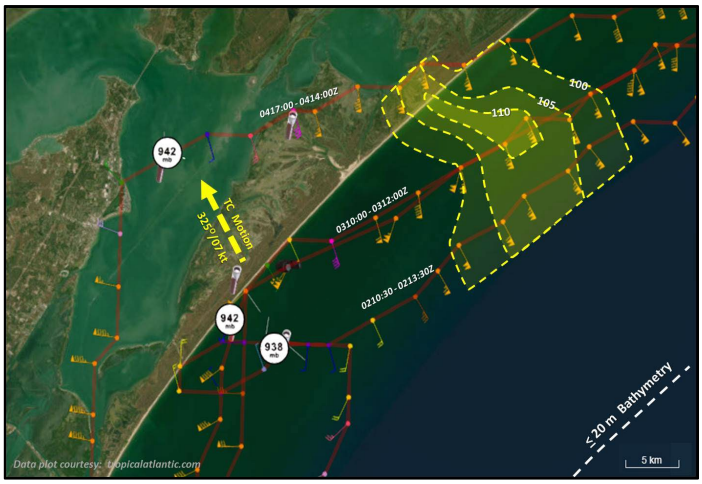

Figure 13. Composite analysis of ESW speeds (kt; yellow dashed and shaded areas) derived from applying the 0.90 adjustment factor to 700-hPa aircraft flight-level wind speeds (kt) during three USAFR legs from 0210:30–0213:30Z, 0310:00–0312:00Z, and 0417:00–0414:00Z 26 August 2017 as Harvey was making landfall along the Texas coast. (Reconnaissance data plot courtesy of *tropicalatlantic.com*)

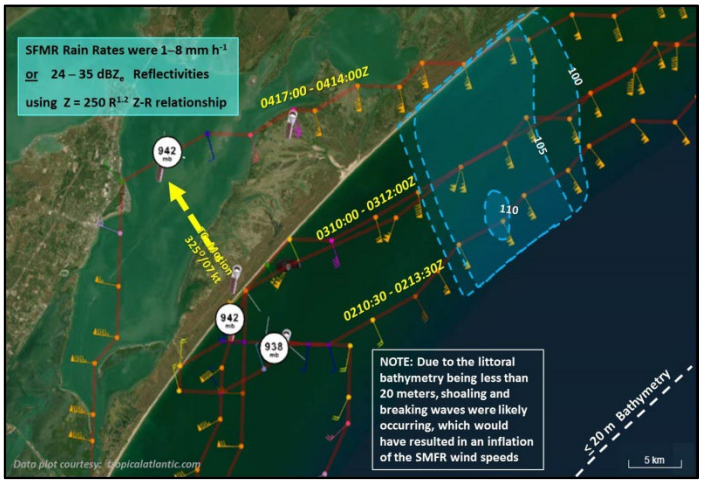

Figure 14. Composite analysis of SFMR 10-meter wind speeds (kt) during three USAFR legs from 0210:30–0213:30Z, 0310:00–0312:00Z, and 0417:00–0414:00Z 26 August 2017 as Harvey was making landfall along the Texas coast. (Reconnaissance data plot courtesy of *tropicalatlantic.com*)

Although there was one SFMR wind speed value of ~110 kt, the majority of SFMR near-surface wind estimates were 105 kt; the 110-kt estimate and much of the 105-kt wind speed estimates could have been enhanced by breaking waves and shoaling due to the shallow depth (<20 m) of the littoral waters of the central Texas coast. Data from the KCRP WSR-88D Doppler radar also indicated that the strongest flight-level winds of 110-124 kt along and just offshore the Texas coast were associated with relatively weak equivalent reflectivities of 25-35 dBZ$_e$, yielding rainfall rates of 1–8 mm h^{-1} (Fig. 15) based on the WSR-88D tropical Z-R relationship. Moreover, those radar-derived rain rates are supported by the identical SFMR-derived rain rates of 1–8 mmh^{-1}. Both rain rates strongly suggest that downdrafts were likely weak and that a 700-hPa adjustment factor

smaller than 0.90 and closer to 0.85 would have been more appropriate. A lower intensity below category-4 strength is supported by a dropwindsonde released at 0212:00 UTC that sampled the eyewall low-level wind field, yielding identical intensity estimates of 100 kt (51.5 ms^{-1}) based on average wind speeds in the lowest 500 m (MBL – mean boundary layer) and lowest 150 m (WL150) data. Multiple dropwindsondes released earlier in the right semicircle of Harvey's eyewall circulation from 1832–2030 UTC 25 August 2017 yielded even lower surface wind speed estimates of 94–99 kt (48.4–51.0 ms^{-1}).

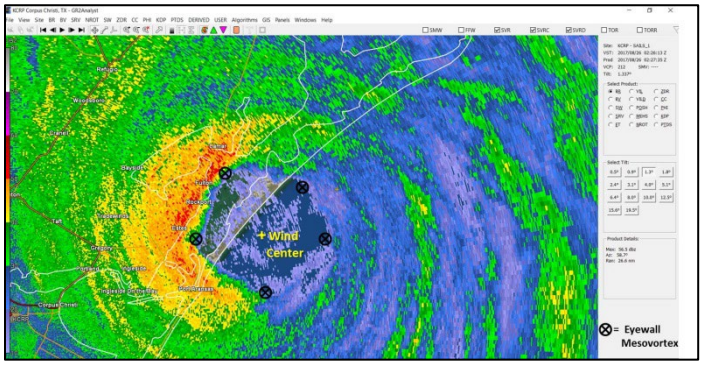

Figure 15. Corpus Christi, TX (KCRP) WSR-88D Doppler radar reflectivity data (dBZ_e) at 0227:35 UTC, 26 August 2017 just prior to Harvey making landfall along the Texas coast. There were at least five well-defined mesocyclones (black circled-X) embedded within the eyewall. Note the weak reflectivity values over the Gulf of Mexico northeast through south of the wind center (yellow cross) where peak 700-hPa aircraft flight-level winds of 119–124 kt (61.3–63.9 ms^{-1}) were located. (Radar data display courtesy *grlevelx.com*)

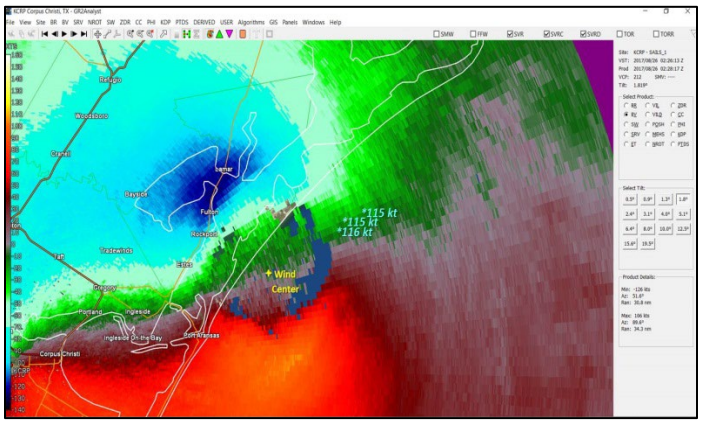

Figure 16. Corpus Christi, TX (KCRP) WSR-88D Doppler radar base velocity data (kt) at 0227:35 UTC, 26 August 2017 for the 1.8° elevation angle, which equates to an altitude range of 9,600–10,600 ft (2,927–3,232 m) ASL over water. Peak $4BAV_{TANGENTIAL}$ wind speeds of 115–116 (kt) support the aircraft 700-hPa flight-level winds at those locations over water (light-blue text). Strong Doppler velocity values of 120–126 kt (dark-blue region) are indicated over land just north of Fulton, TX. (Radar data display courtesy *grlevelx.com*)

The landfall intensity estimate of 105–110 kt (54.1–56.7 ms^{-1}) proposed in this research is similar to an intensity estimate obtained by Alford et al (2019a) based on dual-Doppler analyses of C-band (5-cm wavelength) Shared Mobile Atmospheric Research and Teaching (SMART) radar data and the Corpus Christi, TX (KCRP) WSR-88D Doppler weather radar, which indicated that, "…at most, [Harvey was] a Category 3 hurricane [with] 50–58 ms^{-1} [97–112 kt] sustained winds at landfall."

Their study also indicated that multiple mesovortices in the inner eyewall of Hurricane Harvey (e.g., Figure 15) produced the strongest flow observed in the hurricane. One of the most intense eyewall mesovortices (EMV) also possessed a tornadic vortex signature (TVS) also that later produced significant damage near Fulton and Rockport, TX (Figure 17). That vertically shallow TVS developed within Harvey's northern eyewall located just offshore the Texas coastline over the western Gulf of Mexico around 0100 UTC 26 August 2017 and propagated southwestward to a location along the coastline of South Padre Island by 0114:58 UTC where the TVS achieved a maximum

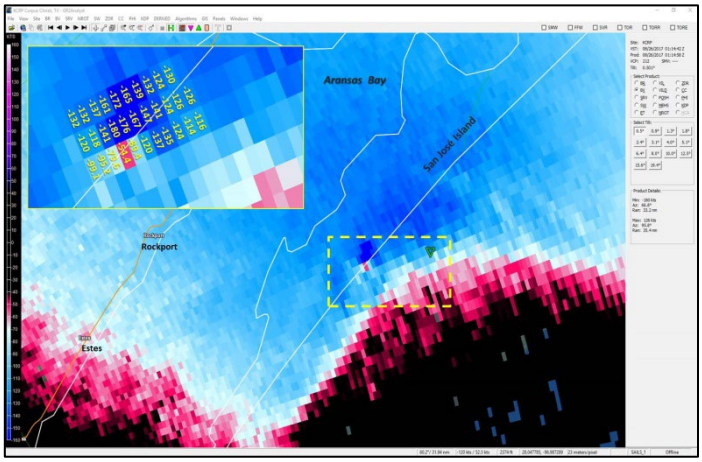

Figure 17. Corpus Christi, TX (KCRP) WSR-88D Doppler radar base velocity data (kt) at 0114:58 UTC, 26 August 2017 for the 0.5° elevation angle. An intense tornadic vortex signature (TVS) is located along the coastline of South Padre Island, TX (yellow-dashed box) at an altitude of 2,606 ft (748 m) ASL. Peak velocity (inset image) within the TVS was 180 kt (92.8 ms^{-1}). (Radar data display courtesy *grlevelx.com*)

inbound (i.e., negative value) intensity of -180 kt (-92.8 ms^{-1}) at an altitude of 2,606 ft (748 m) ASL. The adjacent radial data bin possessed an inbound Doppler velocity value of -54.4 kt (28.0 ms^{-1}), yielding an extreme radial gate-to-gate $\Delta V_{DOPPLER}$ of 125.6 kt (64.7 ms^{-1}). The magnitude of that low-level velocity difference (LLVD) is frequently associated with tornadoes ≥EF-2 intensity (LaDue et al 2012). Obviously, wind speeds associated with a TVS, EMV, or other non-tangential eyewall perturbation has to be filtered out to avoid overestimating a TC's true intensity.

5. CONCLUSIONS

(1) The proposed $4BAV_{ACTUAL}$ (or $4BAV_{TANGENTIAL}$) technique compares extremely well with USAFR and NOAA reconnaissance aircraft flight-level 10-s average wind speed data based on the correlation coefficient of 0.99 and the relatively small root-mean square error (RMSE) of 3.69 kt. This indicates excellent fidelity between the aircraft-derived flight-level wind speeds and the radar-derived 4BAV-derived V_{ACTUAL} wind speeds.

(2) When Hurricane Katrina made landfall in southeastern Louisiana in the early morning hours of 26 August 2005, $4BAV_{ACTUAL}$ (or $4BAV_{TANGENTIAL}$) wind speed values yielded equivalent 10-m wind speeds of 126–130 kt (65–67 ms^{-1}) or Category 4 strength, vice the post-analysis assessed Category-3 intensity of 110 kt (56.5 ms^{-1}).

(3) As Hurricane Katrina made landfall near the Louisiana-Mississippi border in the late morning hours of 26 August 2005, $4BAV_{ACTUAL}$ (or $4BAV_{TANGENTIAL}$) wind speed values yielded equivalent 10–m wind speeds of 114–118 kt (65–67 ms^{-1}) or Category–4 strength, vice the post-analysis assessed Category–3 intensity of 105 kt (54.1 ms^{-1}).

(4) When Hurricane Harvey made landfall along the central Texas coast northeast of Corpus Christi, during early evening hours of 25 August 2017, $4BAV_{ACTUAL}$ (or $4BAV_{TANGENTIAL}$) wind speed values yielded

equivalent 10-m wind speeds of 105 kt (54.1 ms^{-1}) to no more than 110 kt (56.7 ms^{-1}) or Category 3 strength, vice the post-analysis assessed Category-4 intensity of 110 kt (56.5 ms^{-1}).

(5) A comparison of dropwindsonde and $4BAV_{TANGENTIAL}$ wind speeds to land-based WSR-88D Doppler radar equivalent radar reflectivity data suggest that a minimum value of 35-36 dBZ_e is required to produce downdrafts strong enough to utilize the the NHC's 0.90 700-hPa flight-level-to-surface wind speed adjustment factor.

(6) Wind speeds associated with a TVS, EMV, or other non-tangential eyewall perturbation must be filtered out to avoid overestimating a TC's true intensity.

6. REFERENCES

Alford, A.A., Biggerstaff, M.I., Carrie, G.D., Schroeder, J.L., Hirth, B.D. and Waugh, S.M. (2019a) Near-surface maximum winds during the landfall of Hurricane Harvey. *Geophysical Research Letters*, **46**, 973–982.

Beven, J. and Cobb, H., 2014: *NOAA-National Hurricane Center Tropical Cyclone Report on Hurricane Irene (2003)*. (https://www.nhc.noaa.gov/data/tcr/AL132003_Isabel.pdf)

Black, M. L., and Franklin J. L., 2000: GPS dropsonde observations of the wind structure in convective and non-convective regions of the hurricane eyewall. Preprints, 24th Conf. on Hurricanes and Tropical Meteorology, Fort Lauderdale, FL, *Amer. Meteor. Soc.*, 448–449.

Blake, E. and Zelinsky, D., 2018: *NOAA-National Hurricane Center Tropical Cyclone Report on Hurricane Harvey (2017)*. (https://www.nhc.noaa.gov/data/tcr/AL092017_Harvey.pdf)

Velden, Christopher; Bruce Harper; Frank Wells; John L. Beven II; Ray Zehr; Timothy Olander; Max Mayfield; Charles "Chip" Guard; Mark Lander; Roger Edson; Lixion Avila; Andrew Burton; Mike Turk; Akihiro Kikuchi; Adam Christian; Philippe Caroff, and Paul McCrone, 2006: "The Dvorak Tropical Cyclone Intensity Estimation Technique: A Satellite-Based Method That Has Endured For Over 30 Years". *Bull. Amer. Meteor. Soc,.* **87 (9)**: 1195–1214.

Fernandez-Caban, P.L., Alford, A.A., Biggerstaff, M.I., Carrie, G.D., Hirth, B., Kosiba, K., et al., 2019: Observing Hurricane Harvey's eyewall at landfall. *Bull. Amer. Meteor. Soc.*, 100 (5): 759–775.

Franklin, J. L., Black M. L. , and Valde K., 2000: Eyewall wind profiles in hurricanes determined by GPS dropwindsondes. Preprints, 24th Conf. on Hurricanes and Tropical Meteorology, Fort Lauderdale, FL, *Amer. Meteor. Soc.*, 446–447.

Joint Typhoon Warning Center (JTWC), Guam — Tropical Cyclone Report on Super Typhoon Ed (1993). https://www.metoc.navy.mil/jtwc/products/atcr/1993atcr.pdf

Jorgensen, D. P., 1984: Mesoscale and convective scale characteristics of mature hurricanes. Part II: Inner core structure of Hurricane Allen (1980). *J. Atmos. Sci*., **41** , 1287–1311.

Knabb, R. D., J. R. Rhome, and D. P. Brown, 2023: *NOAA-National Hurricane Center Tropical Cyclone Report on Hurricane Katrina (2005)*. (https://www.nhc.noaa.gov/data/tcr/AL122005_Katrina.pdf).

James G. LaDue1, J. G., K. Ortega, B. Smith, G. Stumpf, and D. Kingfield, 2012: A comparison of high resolution tornado surveys to Doppler radar observed vortex parameters: 2011-2012 case studies. Preprints, Sessions 6.3, 26th Conference on Severe Local Storms, Nashville, TN, *Amer. Meteor. Society*.

Lee, W.-C., F. D. Marks, and R. E. Carbone, 1994: Velocity Track Display—A technique to extract real-time tropical cyclone circulations using a single airborne Doppler radar. *J. Atmos. Oceanic Technol*., **11**, 337–356.

Lee, W.-C., B. J. D. Jou, P. L. Chang, and S. M. Deng, 1999: Tropical Cyclone Kinematic Structure Retrieved from Single-Doppler Radar Observations. Part I: Interpretation of Doppler Velocity Patterns and the GBVTD Technique. *Mon. Wea. Rev*., **127**, 2419–2439.

Stewart, S. R., and S. W. Lyons, 1996: A WSR-88D radar view of Tropical Cyclone Ed. *Wea. & Forecasting*, **11**, 115–135.

Uhlhorn, E. W., and D. S. Nolan, 2012: Observational undersampling in tropical cyclones and implications for estimated intensity. *Mon. Wea. Rev.*, **140**, 825–840

Wood, V. T., and R. A. Brown, 1992: Effects of radar proximity on single-Doppler velocity signatures of axisymmetric rotation and divergence. *Mon. Wea. Rev*., **120**, 2798–2807.

Wingo, S. M., and K.R. Knupp, 2016: Kinematic structure of mesovortices in the eyewall of Hurricane Ike (2008) derived from ground-based dual-Doppler analysis. *Mon. Wea. Rev*., **144 (11)**, 4245–4263.

Wurman, J., and K. Kosiba, 2018: The role of small-scale vortices in enhancing surface winds and damage in Hurricane Harvey. *Mon. Wea. Rev*., **146**, 713–722

Session 9B.3, 36th Conference on Hurricanes and Tropical Meteorology, 06-10 May 2024, Long Beach, CA

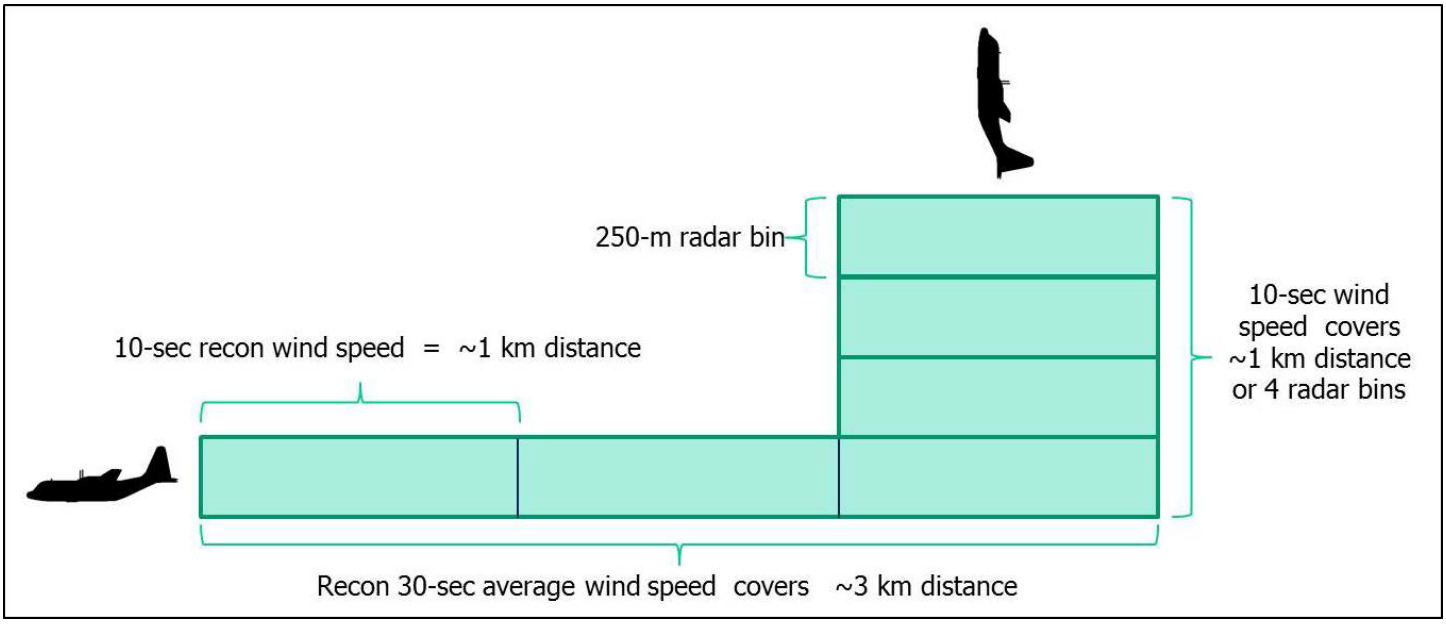

Figure 1. Illustration of reconnaissance aircraft flying 3-km and 1-km lengths that is approximately equal to a 30-second and 10-second, respectively, flight-level average wind speed contained in the High Density Observations (HDOB) Bulletin. NOAA-National Weather Service WSR-88D Doppler weather radar collects radial velocity and velocity spectrum width data at 250-m intervals (bins), with 4 contiguous 'bins' equaling a 1-km-long flight leg.

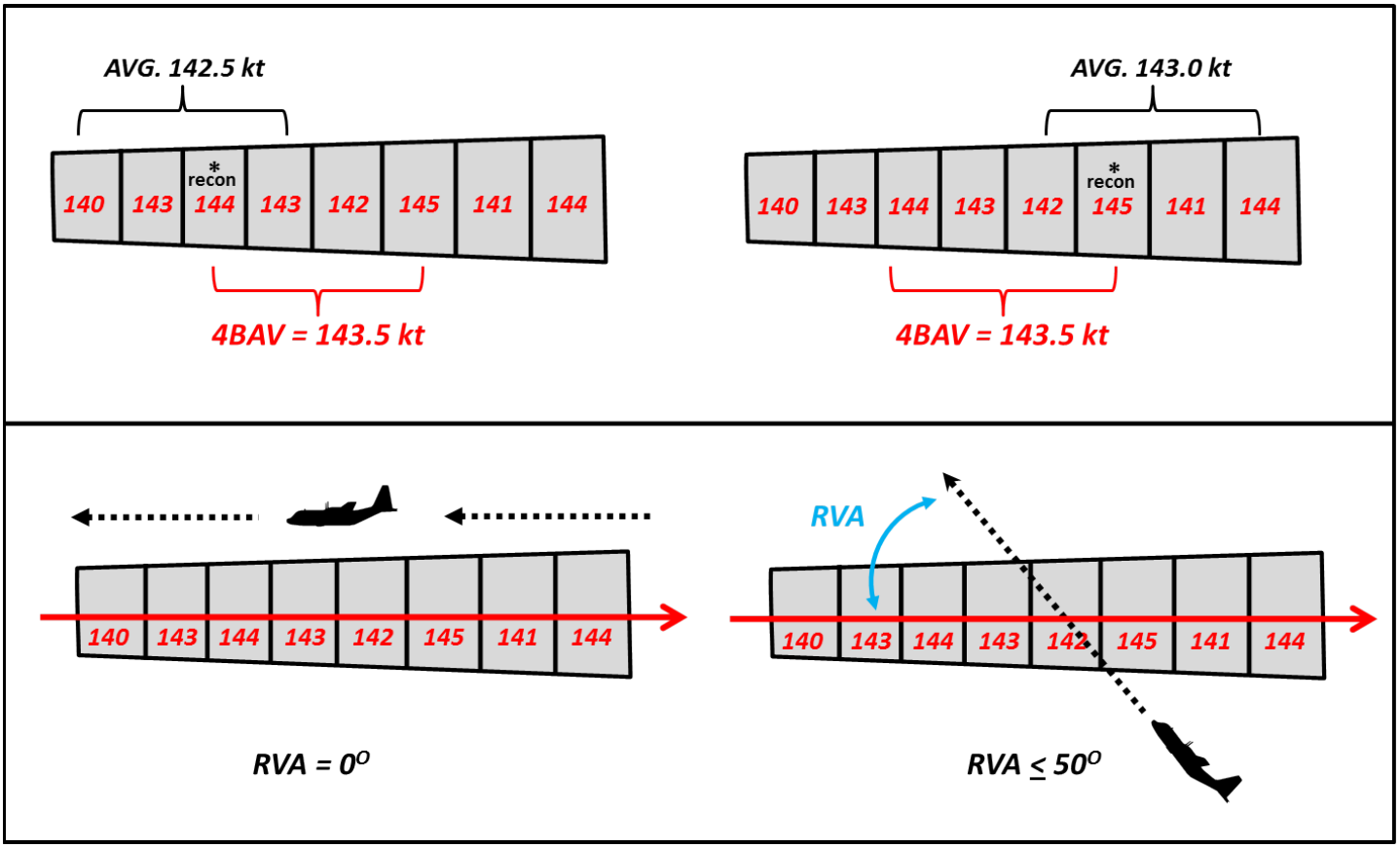

Figure 2. Schematic of a 4-bin average Doppler velocity (4BAV) used to convert to a V_{ACTUAL} wind speed value (top panel). Notice that when RVAs exceed 50^{O}, the aircraft might only sample one or two radar bins of velocity data instead of four bins (bottom panel).

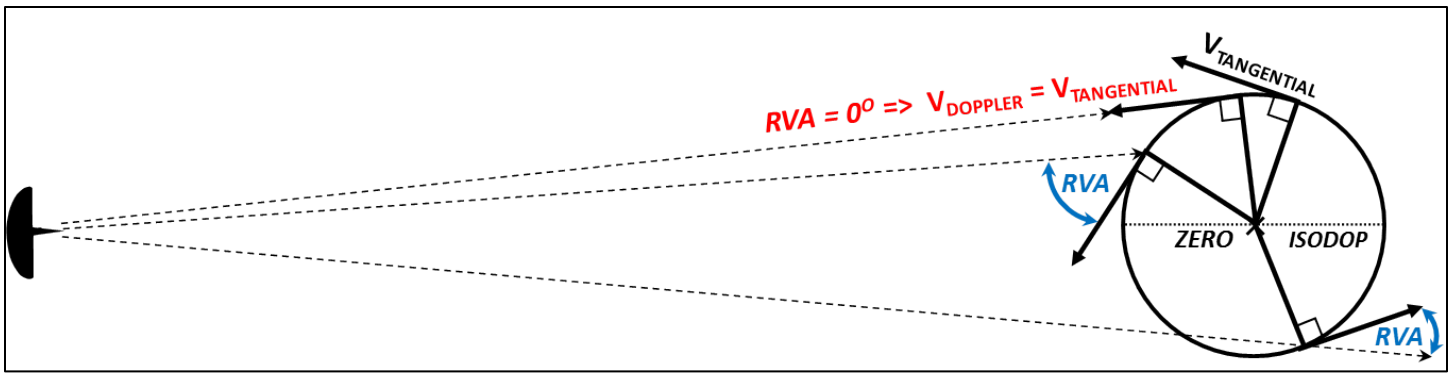

Figure 3. Schematic of various Doppler radar (velocity) viewing angles (RVA). When the RVA is 0^O (i.e., radar radial directly along the actual wind direction), $V_{DOPPLER}$ equals V_{ACTUAL} (or $V_{TANGENTIAL}$).

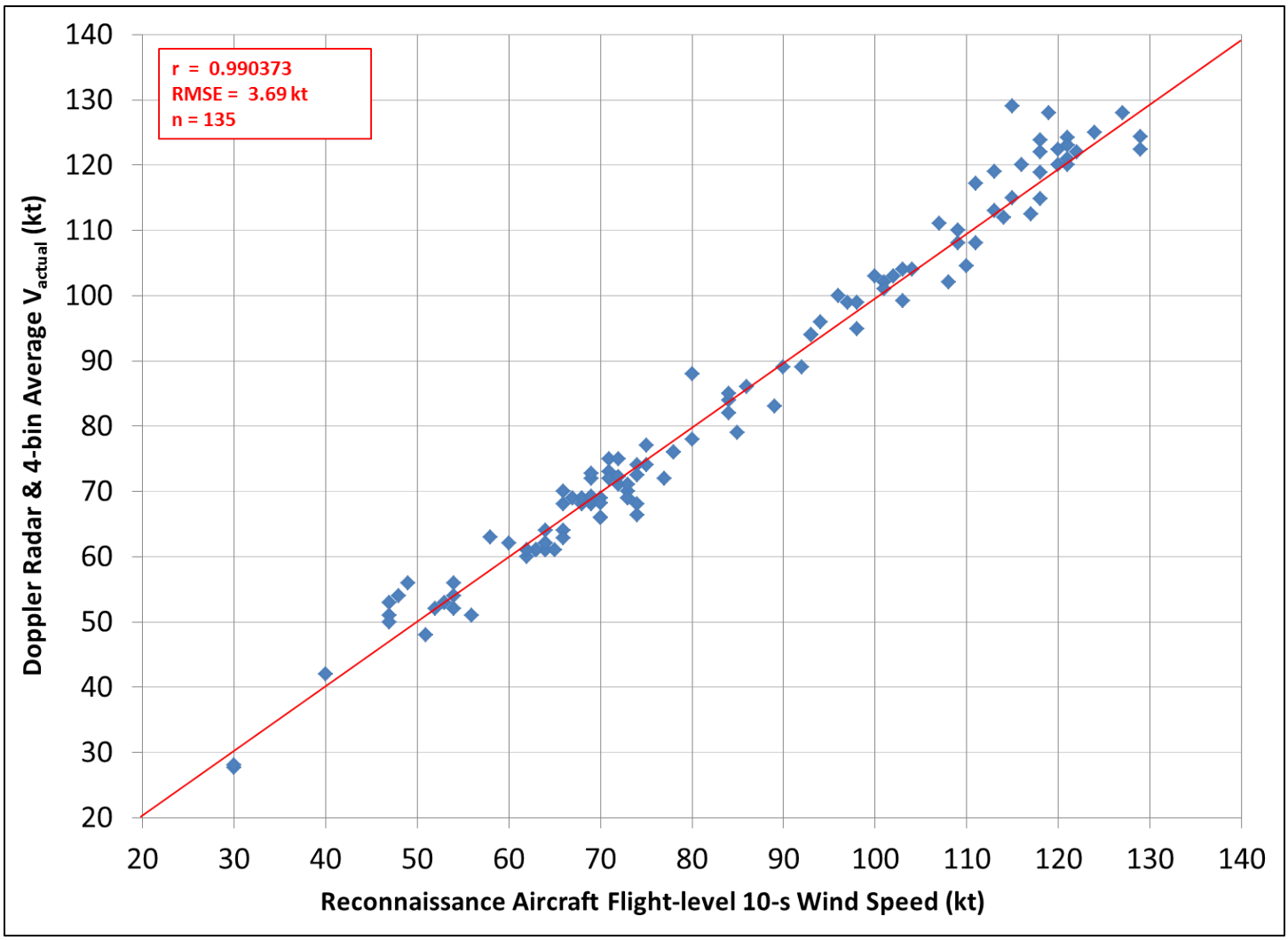

Figure 4. Plot of aircraft 10-second-average flight-level wind speeds (kt) versus V_{ACTUAL} wind speeds (kt) derived from the 4BAV technique. Red line represents a perfect data fit.

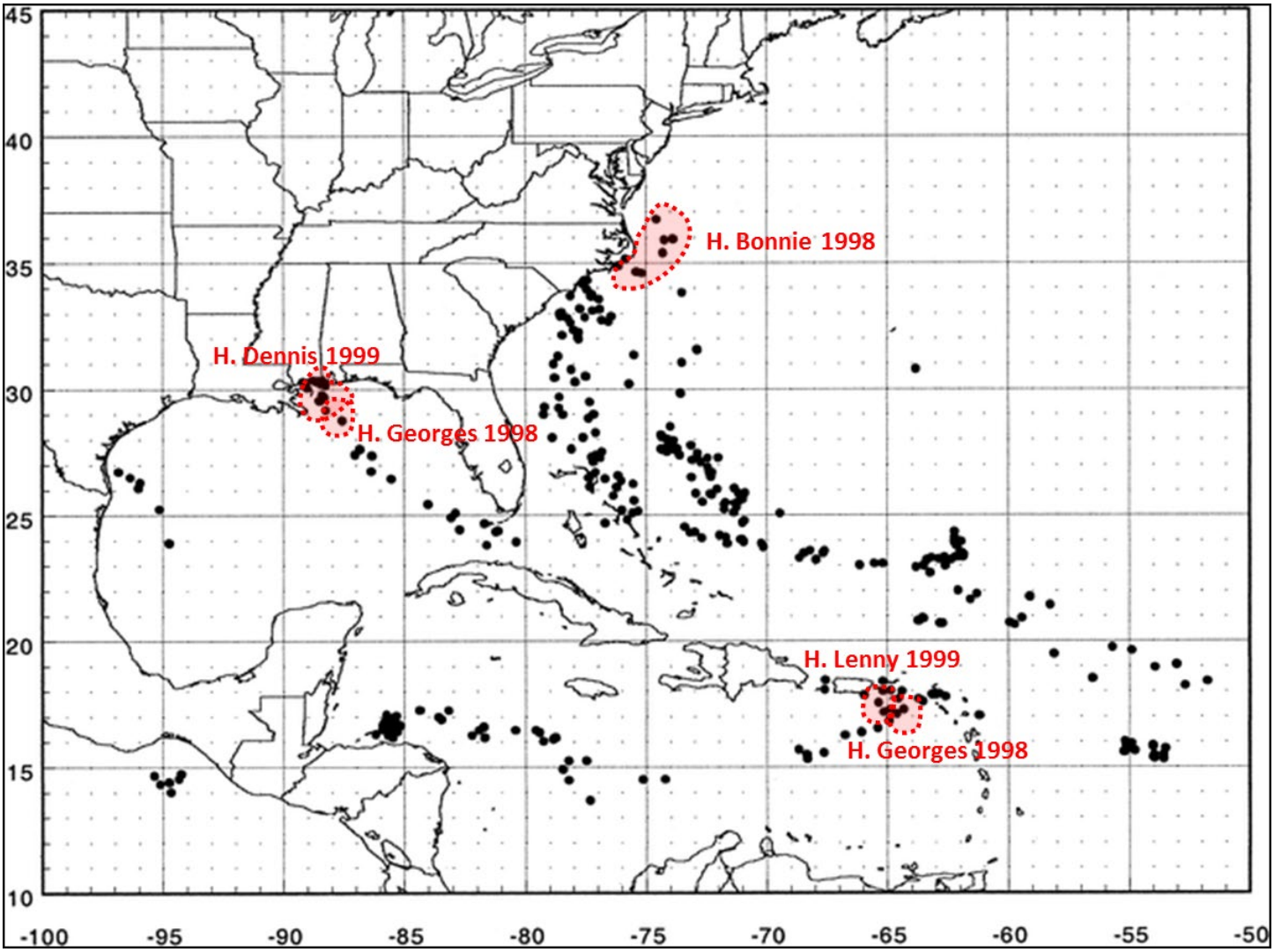

Figure 5. Locations of the 630 dropwindsondes used to derive the adjustment factors shown in Table 2 (Franklin et al 2003, their Figure 1). Red-shaded areas show locations of eyewall dropwindsondes collocated with WSR-88D Doppler weather radar reflectivity data.

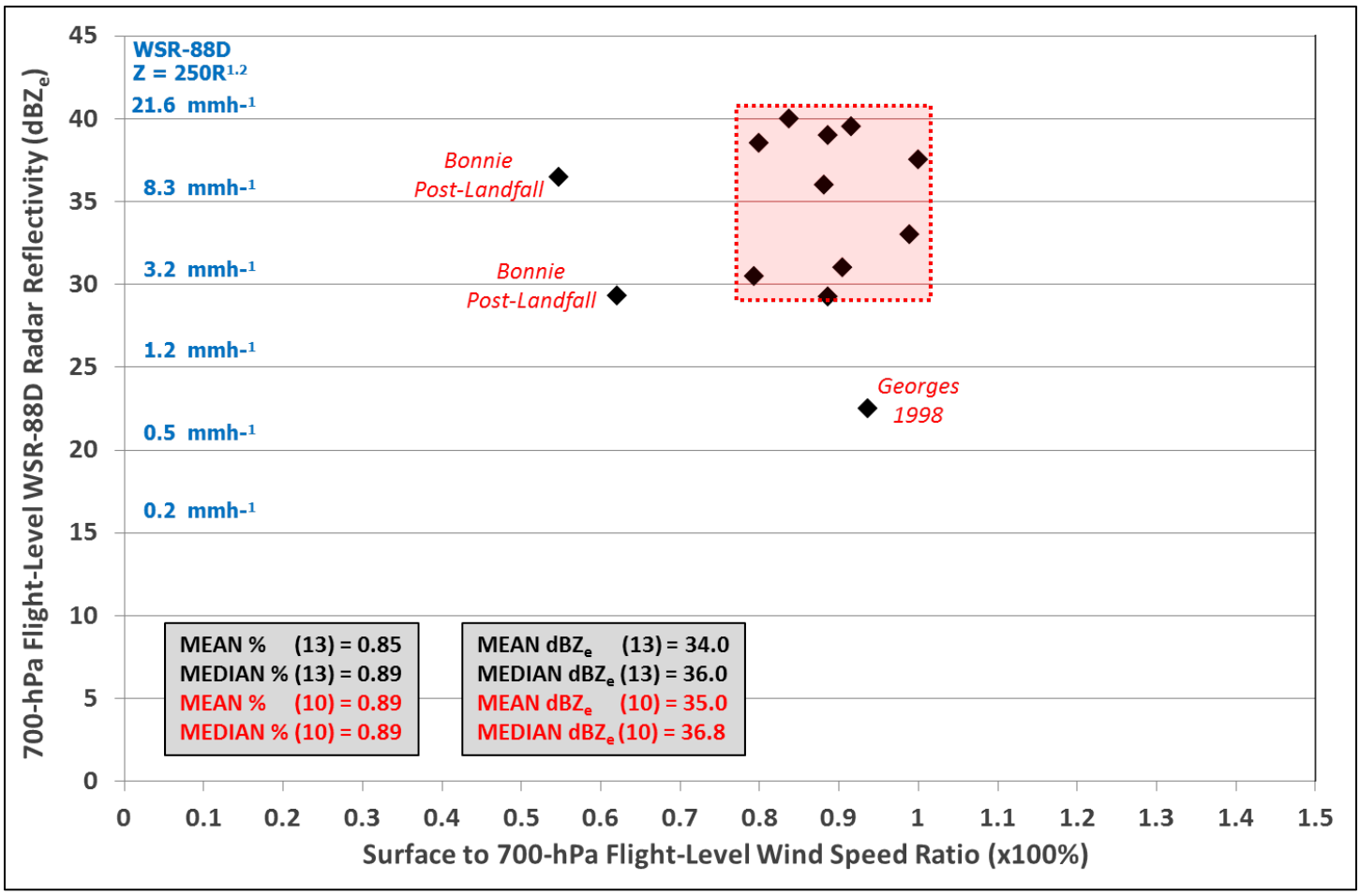

Figure 6. Plot of eyewall surface- to 700-hPa flight-level wind-speed ratios versus 4-bin-average radar reflectivity (dBZ_e) values. Reflectivity datum was collected within ±985 ft (±300 m) of the flight-level RMW altitude (ft).

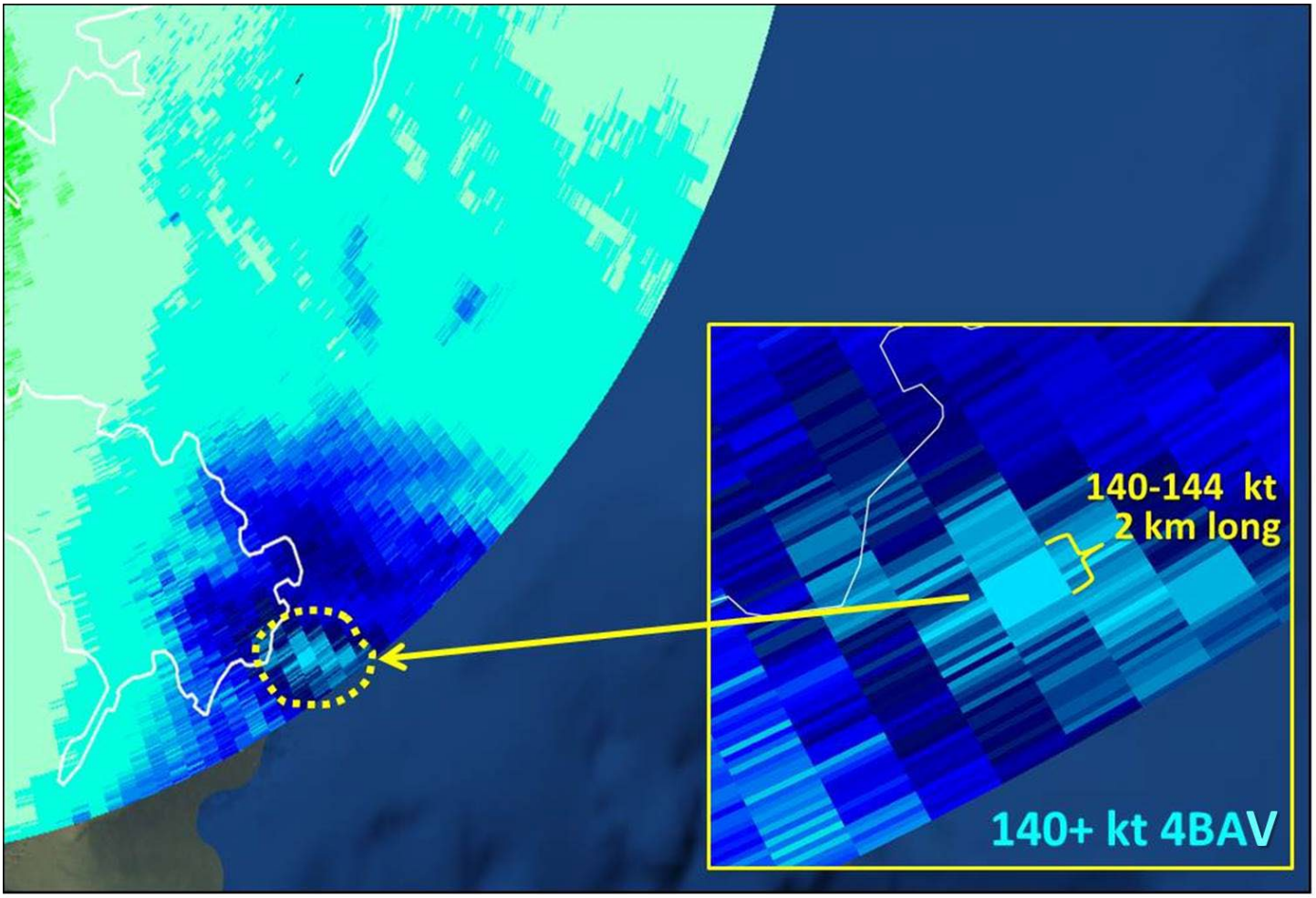

Figure 7. Katrina with a 2-km contiguous run of 140-144 kt $4BAV_{ACTUAL}$ values at ~9,350 ft (2850 m) ASL near landfall over southeastern Louisiana at 0826:48 UTC 29 AUG 2005 from KLIX-Slidell, LA WSR-88D Doppler radar. (radar data display courtesy *grlevelx.com*)

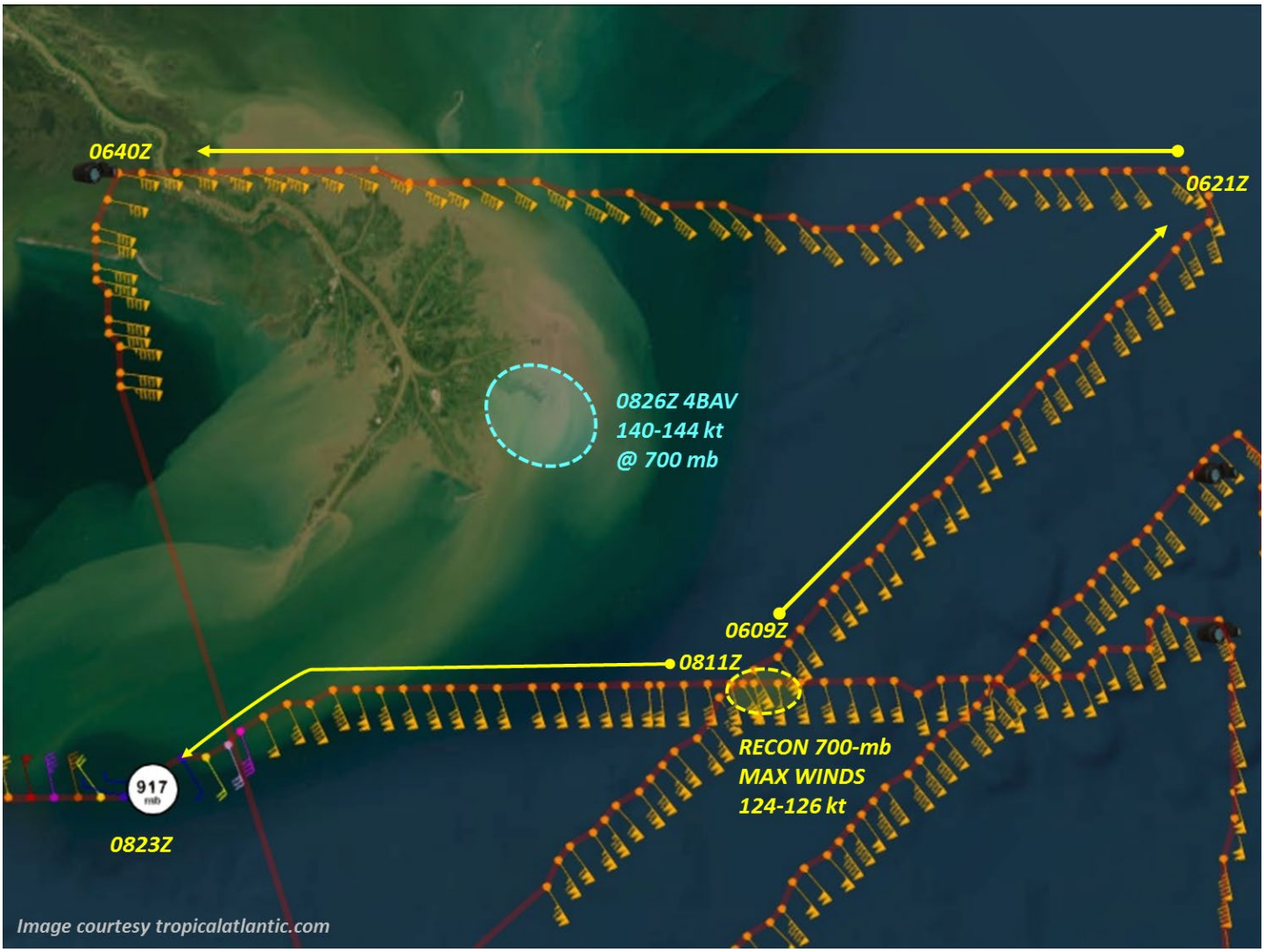

Figure 8. Depiction of the area of 140-144 kt $4BAV_{ACTUAL}$ wind speed values at 0826:48 UTC 29 AUG 2005 and the various flight tracks of an Air Force Reserve reconnaissance aircraft that circumnavigated and missed Katrina's stronger winds at the Mouth of the Mississippi River. (reconnaissance data plot courtesy of *tropicalatlantic.com*)

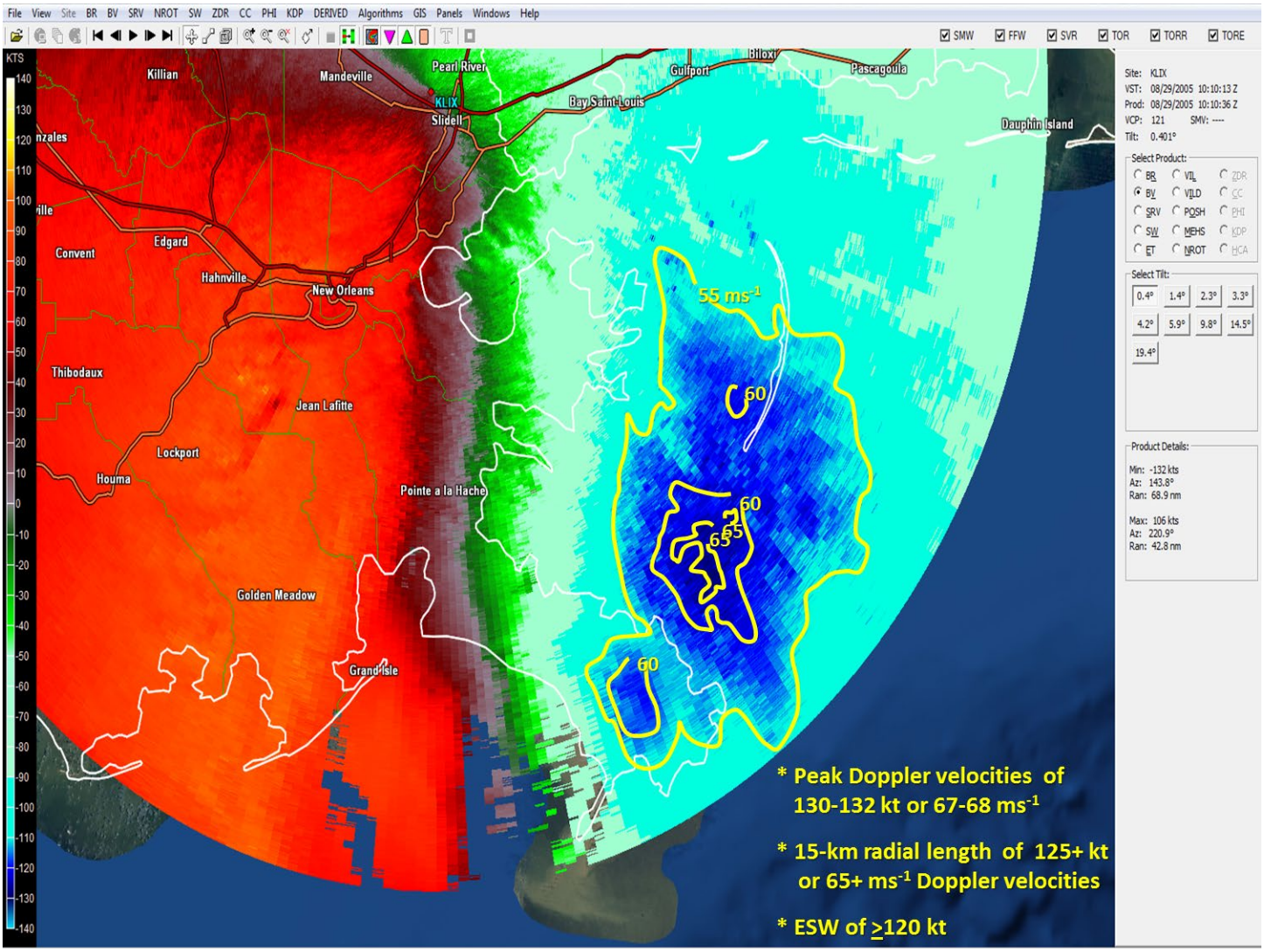

Figure 9. Radar depiction of an area of 116-126 kt 4BAV$_{ACTUAL}$ wind speed values at ~8,500 ft (2600 m) ASL near Louisiana's Chandeleur Islands at 1010:36 UTC 29 AUG 2005 from KLIX-Slidell, LA WSR-88D Doppler radar. (radar data display courtesy *grlevelx.com*)

Figure 10. Depiction of an area of 116-126 kt $4BAV_{ACTUAL}$ wind speed values at 1010:36 UTC 29 AUG 2005 and the various flight tracks of an Air Force Reserve reconnaissance aircraft that circumnavigated and Katrina's stronger winds near Louisiana's Chandeleur Islands. (reconnaissance data plot courtesy of *tropicalatlantic.com*)

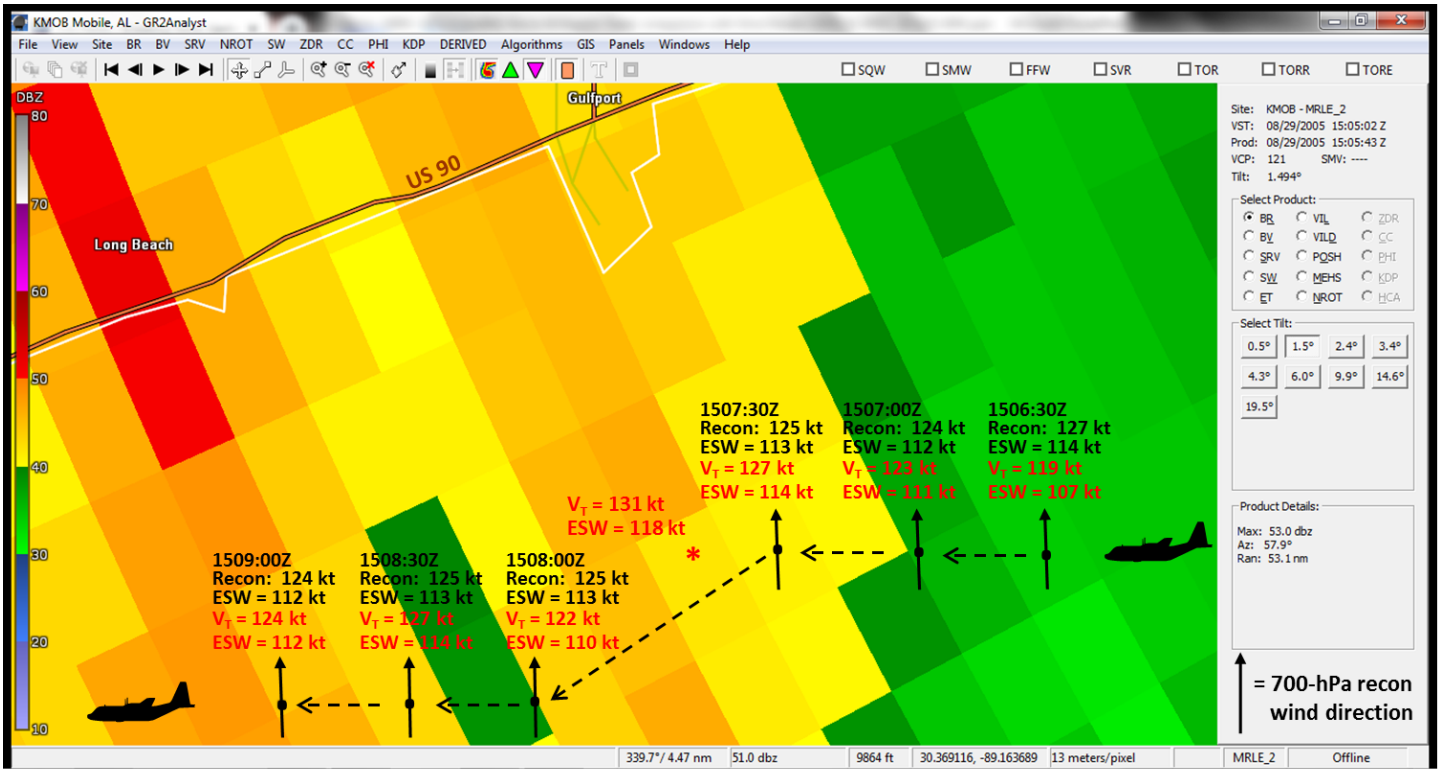

Figure 11. Mobile, AL (KMOB) WSR-88D Doppler radar reflectivity data (dBZ_e) at 1505:43 UTC 29 August 2005 with 1506:30-1509:00 UTC U.S. Air Force Reserve reconnaissance aircraft 700-hPa flight track (dashed black line), flight-level wind speed (kt; black text), flight-level-to-surface equivalent surface wind (ESW) speed (kt; black text), and flight-level wind direction (black arrows; true north at top of image) overlaid. The $4BAV_{TANGENTIAL}$ winds (kt; red text) are within ±1.0 Kft (305 m) of the aircraft flight-level altitude. (radar data display courtesy *grlevelx.com*)

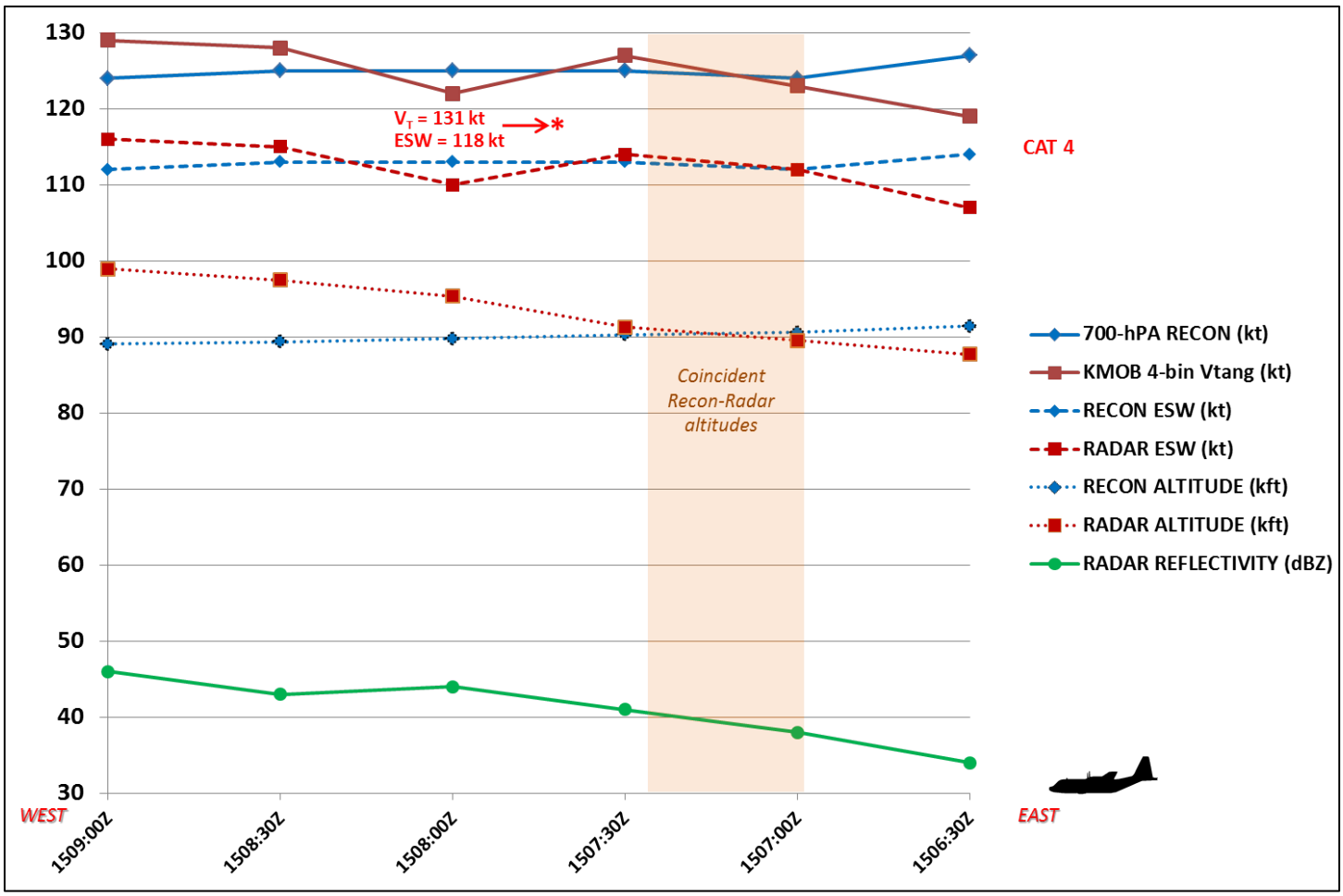

Figure 12. Time series plot of reconnaissance aircraft 700-hPa flight-level data and KMOB WSR-88D Doppler radar reflectivity (dBZ_e), $4BAV_{TANGENTIAL}$ (4-bin V_{tang}) wind data, and radar beam centerline altitude (kft) displayed in Fig. 11 on 29 August 2005.

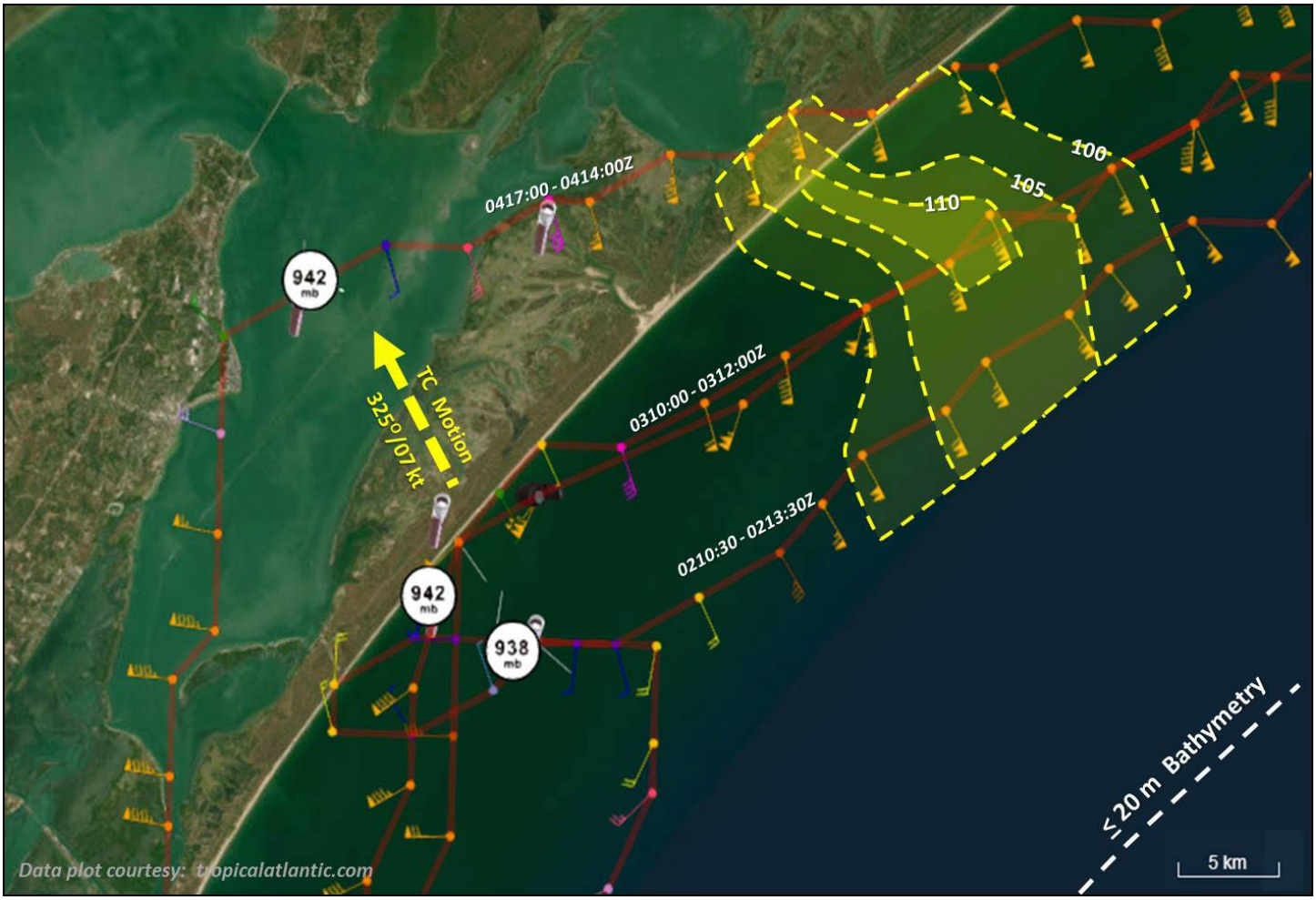

Figure 13. Composite analysis of ESW speeds (kt; yellow dashed and shaded areas) derived from applying the 0.90 adjustment factor to 700-hPa aircraft flight-level wind speeds (kt) during three USAFR legs from 0210:30–0213:30Z, 0310:00–0312:00Z, and 0417:00–0414:00Z 26 August 2017 as Harvey was making landfall along the Texas coast. (reconnaissance data plot courtesy of *tropicalatlantic.com*)

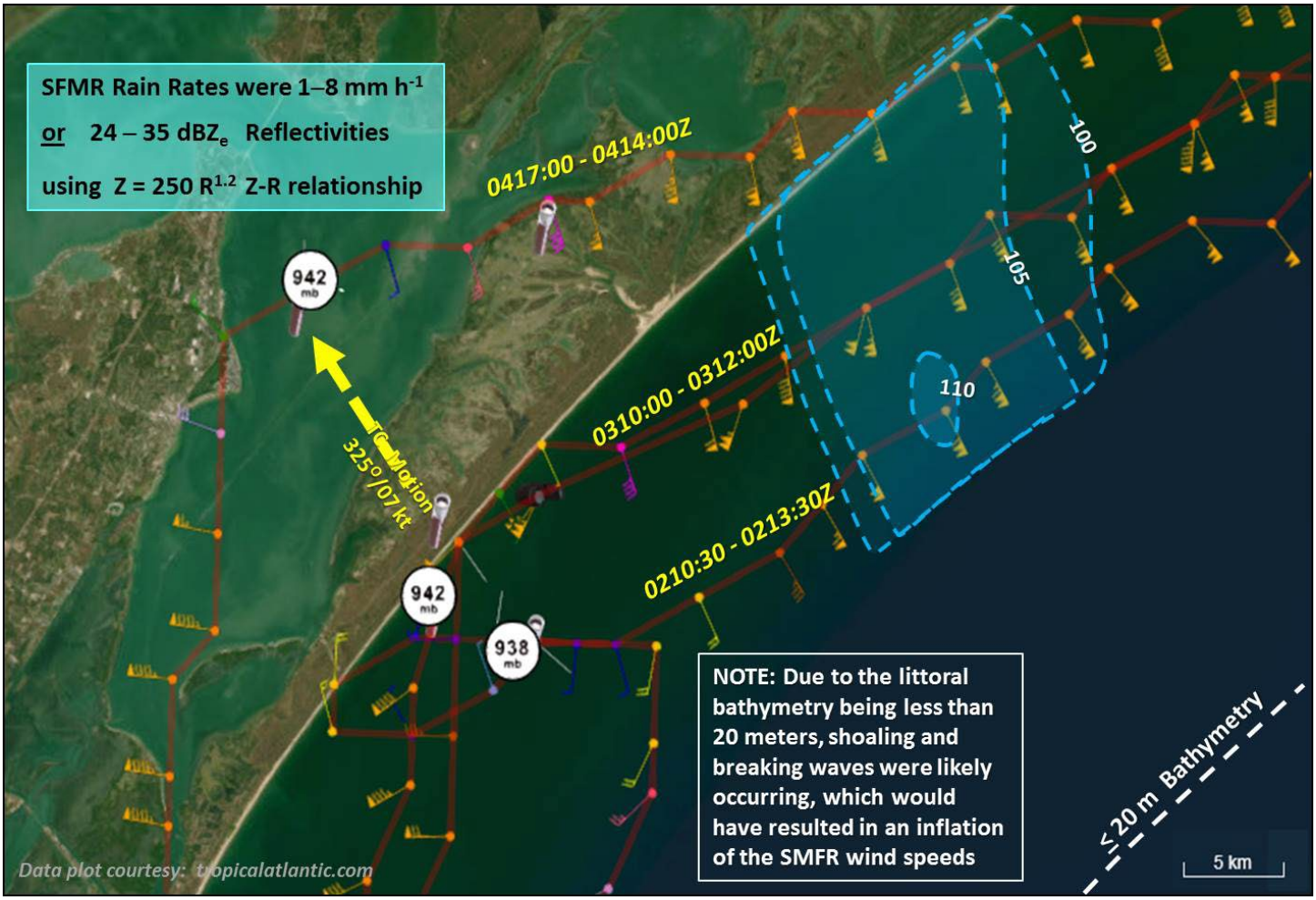

Figure 14. Composite analysis of SFMR 10-meter wind speeds (kt), (yellow dashed and shaded areas) derived from applying the 0.90 adjustment factor to 700-hPa aircraft flight-level wind speeds during three USAFR legs from 0210:30–0213:30Z, 0310:00–0312:00Z, and 0417:00–0414:00Z 26 August 2017 as Harvey was making landfall along the Texas coast. (reconnaissance data plot courtesy of *tropicalatlantic.com*)

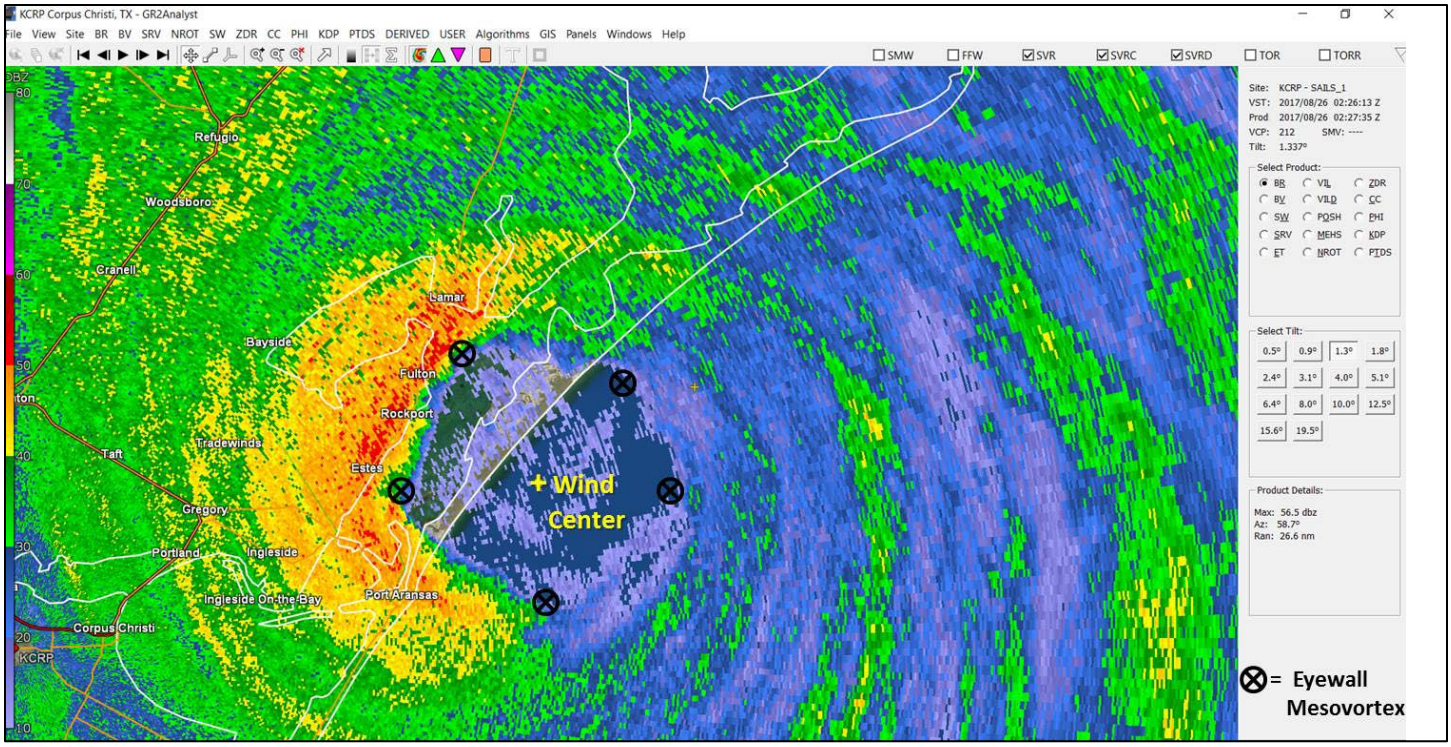

Figure 15. Corpus Christi, TX (KCRP) WSR-88D Doppler radar reflectivity data (dBZ_e) at 0227:35 UTC, 26 August 2017 just prior to Harvey making landfall along the Texas coast. There were at least five well-defined mesocyclones (black circled-X) embedded within the eyewall. Note the weak reflectivity values over the Gulf of Mexico northeast through south of the wind center (yellow cross) where peak 700-hPa aircraft flight-level winds of 119–124 kt (61.3–63.9 ms^{-1}) were located. (radar data display courtesy *grlevelx.com*)

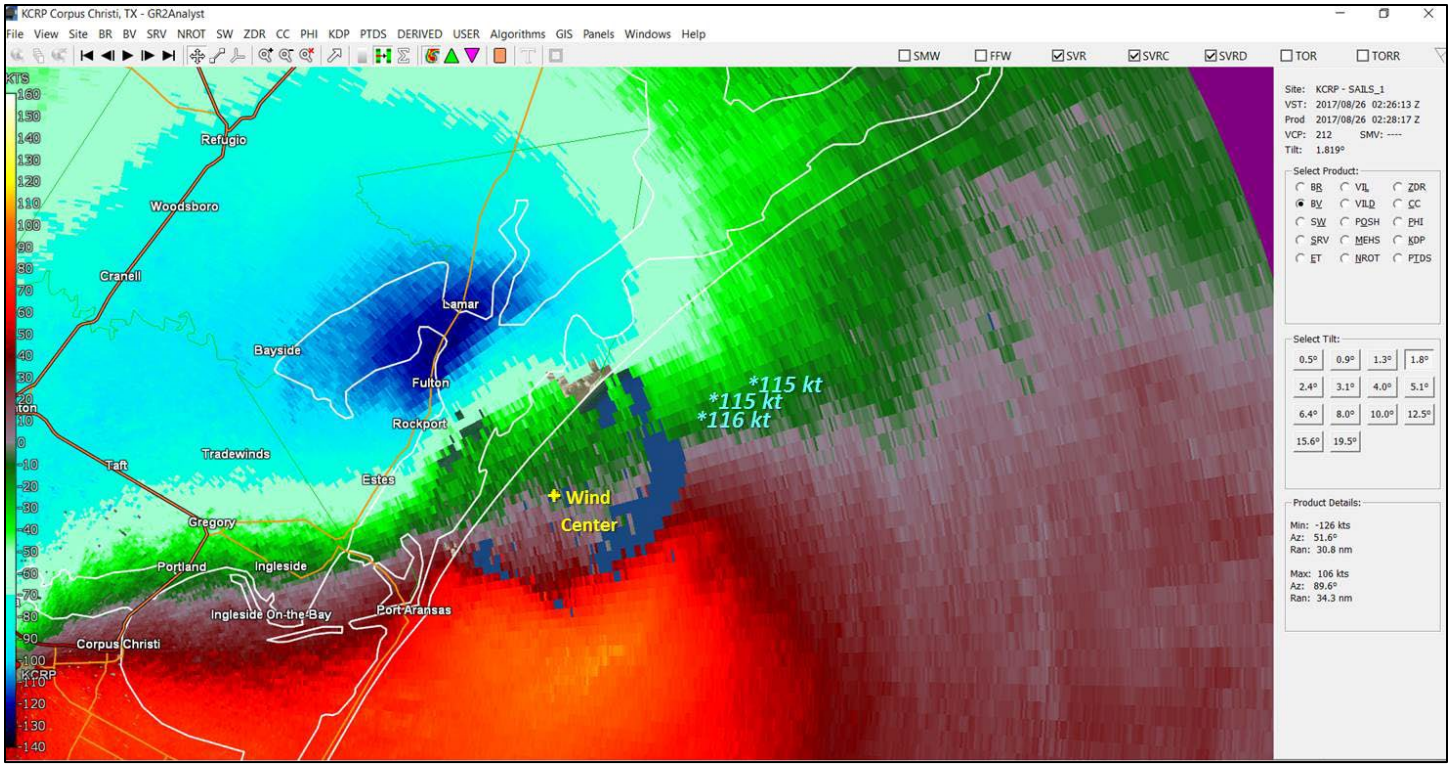

Figure 16. Corpus Christi, TX (KCRP) WSR-88D Doppler radar base velocity data (kt) at 0227:35 UTC, 26 August 2017 for the 1.8^{O} elevation angle, which equates to an altitude range of 9,600–10,600 ft (2,927–3,232 m) ASL over water. Peak 4BAV$_{TANGENTIAL}$ wind speeds of 115–116 (kt) support the aircraft 700-hPa flight-level winds at those locations over water (light-blue text). Strong Doppler velocity values of 120–126 kt (dark-blue region) are indicated over land just north of Fulton, TX. (radar data display courtesy *grlevelx.com*)

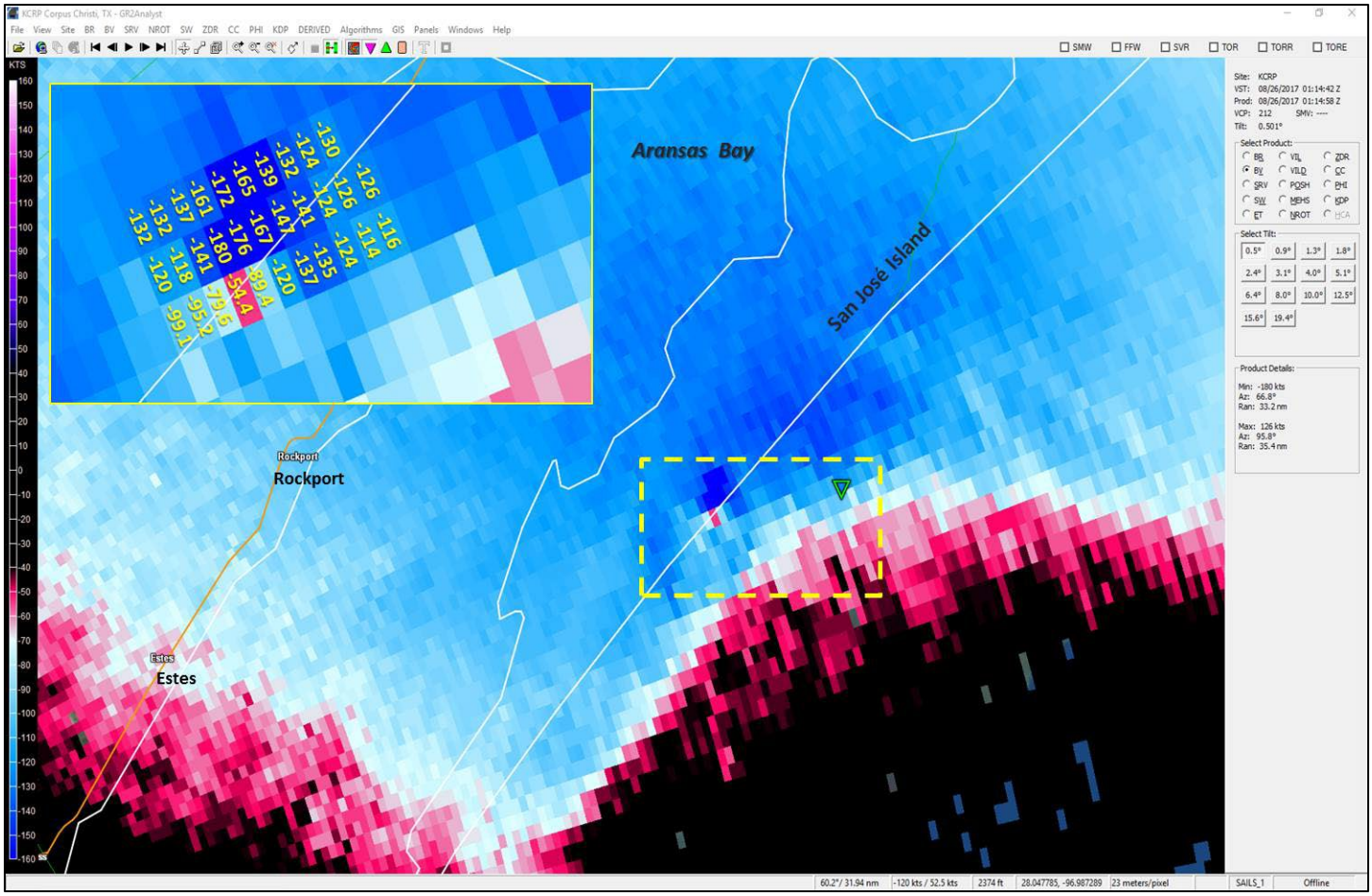

Figure 17. Corpus Christi, TX (KCRP) WSR-88D Doppler radar base velocity data (kt) at 0114:58 UTC, 26 August 2017 for the 0.5^{O} elevation angle. An intense tornadic vortex signature (TVS) is located along the coastline of South Padre Island, TX (yellow-dashed box) at an altitude of 2,606 ft (748 m) ASL. Peak velocity (inset image) within the TVS was 180 kt (92.8 ms^{-1}). (radar data display courtesy *grlevelx.com*)

$4BAV_{DOPPLER}$ (kt) Conversion to $V_{TANGENTIAL}$ (kt) for Various Radar Viewing Angles (RVA)												
$4BAV_{DOPPLER}$ (kt) \ RVA	5^O	10^O	15^O	20^O	25^O	30^O	35^O	40^O	45^O	50^O	55^O	60^O
20									28	31	35	40
30			31	32	33	35	37	39	42	47	52	60
40		41	41	43	44	46	49	52	57	62	70	80
50		51	52	53	55	58	61	78	71	78	87	100
60		61	62	64	66	69	73	78	85	93	105	120
70		71	72	74	77	81	85	91	99	109	122	140
80		81	83	85	88	92	98	104	113	124	139	160
90		91	93	96	99	104	110	117	127	140	157	180
100		102	104	106	110	115	122	131	141	156	174	200
110		112	114	117	121	127	134	144	156	171	192	220
120		122	124	128	132	139	146	157	170	187	209	240
130		132	135	138	143	150	159	170	184	202	227	260
140	141	142	145	149	154	162	171	183	198	218	244	
150	151	152	155	160	177	173	183	196	212	233	262	

Table 1. Nomogram of $V_{TANGENTIAL}$ (V_{ACTUAL}) wind speeds (kt) as a function of $4BAV_{DOPPLER}$ velocity values (kt) and Radar Viewing Angles (RVA).

Flight level	Eyewall	Outer Vortex (convection)	Outer Vortex (not in convection)
700 hPa	0.90	0.85	0.80
850 hPa	0.80	0.80	0.75
925 hPa	0.75	0.75	0.75
1000 ft (305 m)	0.80	0.80	0.80

Table 2. Reconnaissance aircraft flight-level-to-surface (10 m ASL) wind speed adjustment factors (Table 2 from Franklin et al 2003).